

Project Number: JMS-0112

DESIGN AND ANALYSIS OF AN ABSORPTION REFRIGERATION SYSTEM

A Major Qualifying Project Report

Submitted to the Faculty

Of the

WORCESTER POLYTECHNIC INSTITUTE

in partial fulfillment of the requirements for the

Degree of Bachelor of Science

in Mechanical Engineering

by

Kajano, Joseph

Lucas, Doug

Muyuka, Glorius

Date: April 26, 2012

Approved:

Professor John M Sullivan, Major Advisor

ABSTRACT

This project focuses on the construction of a three fluid gas absorption refrigeration unit, intended to operate in a 20°C environment, with a compartment temperature of 3°C. Gas absorption systems, unlike vapor-compression systems, use a heat source to facilitate refrigeration. Three fluid gas absorption refrigerators use no electricity and no moving parts, such as pumps and compressors, and operate at a single system pressure. Unlike the vapor-compression cycle, which utilizes pressure gains and drops to produce refrigeration, the three fluid gas absorption cycle uses the principle of partial pressure between two fluids to create the cooling effect. Extensive analysis of the thermodynamics, heat transfer, and chemical properties of a three fluid gas absorption system was conducted to design and construct the structural model shown in the report. This model was pressure tested for structural integrity and leakage and a safety analysis of the fluids involved was undertaken to insure proper functionality when the gases are introduced.

TABLE OF CONTENTS

ABSTRACT	1
TABLE OF FIGURES.....	4
TABLE OF NOMENCLATURE	5
GOAL STATEMENT	7
INTRODUCTION	8
BACKGROUND.....	9
Refrigeration Cycles.....	10
Magnetocaloric Refrigeration System	10
Thermoelectric Refrigeration System	11
The Vapor-Compression Refrigeration System	12
The Absorption Refrigeration System.....	15
Two Fluid Absorption Refrigeration System.....	16
Three Fluid Absorption Refrigeration System	23
System Selection.....	25
SYSTEM ANALYSIS AND DESIGN.....	25
Refrigerant and Third Fluid	25
Material Selection	29
Refrigerator Cabinet	30
Evaporator	41
ABSORBER.....	54
Condenser Analysis.....	55
Generator Analysis	58
System Theoretical Performance	70
DETERMINATION OF MASSES	83
Hydrogen Mass.....	84
Ammonia:.....	85
Liquid Ammonia Hydroxide:.....	86
PART DESCRIPTION.....	87
Part Prices	92
CONSTRUCTION.....	92
FILLING PROCEDURE.....	98

SYSTEM SAFETY	100
TESTING AND MEASURING PROCEDURES	106
Volume Measurement	106
Bubble Pump Testing	107
Pressure Testing	108
RESULTS	108
Liquid solution and total system volume	108
Masses of all fluids	109
Bubble Pump Flow rate	109
Pressure Test	109
CONCLUSION	110
APPENDIX 1	111
APPENDIX 2	112
APPENDIX 3	113
WORKS CITED	115

TABLE OF FIGURES

Figure 1 Heat engine thermodynamic schematic. (Karonen)	9
Figure 2 Magnetocaloric effect on Gadolinium alloy.	11
Figure 3 Thermoelectric plate diagram	12
Figure 4 Vapor-compression system diagram.....	14
Figure 5 Vapor-compression P vs. v diagram.....	14
Figure 6 Vapor-compression T vs. s diagram	15
Figure 7 Ammonia-water single stage absorption refrigeration system flow diagram	18
Figure 8 T vs. s graph of pure ammonia made from data in table 10.	21
Figure 9 P vs. v of pure ammonia constructed from data in table 10.	21
Figure 10 Diagram with state points of a basic three fluid absorption system.	24
Figure 11 simplified model of absorber.....	27
Figure 12 T vs. s diagram of ammonia cycle.	48
Figure 13 T vs. s diagram of ammonia cycle with pre-cooling.....	49
Figure 14 System diagram for accompanying T vs. s chart without pre-cooling	51
Figure 15 Solubility graph of ammonia in water	59
Figure 16 Temperature-concentration diagram of evaporation process.....	63
Figure 17 Enthalpy vs. concentration diagram	64
Figure 18 Enthalpy vs. mass fraction of ammonia	67
Figure 19 COP vs. mass fraction.....	71
Figure 20 Q vs. mass fraction diagram.....	72
Figure 21 Mass flow diagram.....	73
Figure 22 COP with heat exchange. The Max and Min values are listed on the y-axis.	75
Figure 23 Net heat input Q_{net} . Max and Min are labeled.....	75
Figure 24 Heat value of the exiting gases at point 3.	77
Figure 25 COP with heat exchange and solution pre-cooling	78
Figure 26 Net heat input with Heat exchange, and pre-cooling.	79
Figure 27 COP with heat exchange and pre-cooling. However, this chart includes a heat exchanger effectiveness of $\epsilon=0.692$	81
Figure 28 Hand held tube bender	93
Figure 29 File and hacksaw	94
Figure 30 Flaring kit and flared tube end.....	94
Figure 31 Flared T-fitting and junction assembly.....	95
Figure 32 Flared tube connection illustration	96
Figure 33 Picture of completed system	98
Figure 34 Illustration of operating liquid level.....	107

TABLE OF NOMENCLATURE

A = surface area

β = volumetric thermal expansion coefficient

COP = coefficient of performance

D = diameter

ε = heat exchanger effectiveness

g = gravitational acceleration

Gr_L = grashof number of a plate

h = convection coefficient between air and surface

h_{sp} = specific enthalpy

h_1 = convection coefficient rate between air and outer surface at state 1

h_2 = convection coefficient between the inner walls and inside air at state 2

I = electric current

K = conduction coefficient

L = length/distance

m_i = mass of element i

\dot{m} = mass flow rate

ρ_i = density of element i

P = pressure

P_T = total pressure

P_i = partial pressure of element i

Pr = prandlt nuber

Q = heat transfer

R = resistance

Ra = rayleigh number

R_{tot} = total resistance of a heat circuit

s = entropy

Sc = schmidt number

Sh = sherwood number

t_w = wall thickness

T = temperature

T_{∞} = ambient temperature of the air

T_{lm} = logarithmic mean temperature

T_p = temperature within the pipe

T_r = temperature of refrigerator compartment

T_s = surface temperature

μ = viscosity

U = effective coefficient between two fluids

v_i = velocity at point i

v = specific volume

ν = kinematic viscosity

V = electric voltage

X_i = mass fraction of element i

X_{B1} = mole fraction of B some distance L above the liquid interface

X_{B2} = mole fraction of B at the liquid interface

Z = height

GOAL STATEMENT

The goal of this project is to design and fabricate a structurally sound model of a three fluid gas absorption refrigeration system that uses ammonia, water, and hydrogen to maintain a refrigerated compartment temperature of 3°C under an outside ambient temperature of 20°C.

INTRODUCTION

Before the first millennium, the Chinese cooled their food and drinks with harvested ice. The Romans, Greeks, and Hebrews placed large amounts of snow into storage pits dug into the ground covered with wood and straw for insulation. The ancient Egyptians filled earthen jars with boiled water and exposed the jars to the night air for their cooling; and in 1550, cooling of wine by adding chemicals such as sodium nitrate and potassium nitrate to water was first recorded. It was also in those same records that the first use of a word meaning “to refrigerate” appeared (Krasner-Khait).

Refrigeration is the process of cooling a space or substance below environmental temperatures. Refrigeration was done primarily using methods similar to those mentioned above until the initiation of the commercial refrigerator in 1856 by Alexander Twinning. Oliver Evans designed the first refrigeration machine, or refrigerator, in 1805; but it was John Gorrie who produced the first working model. Gorrie created a refrigeration effect by compressing a gas, cooling it through radiating coils, and expanding it to lower the temperature further. It is this method of refrigeration that is most widely used today and is known as the vapor-compression process (Krasner-Khait).

The technological advancements made over the last 100 years have been nothing short of astonishing, but despite all these advancements, the fundamentals of the refrigeration process have remained virtually the same. Modern advancement has given us alternative ways to conduct this refrigeration, in addition to increasing its efficiency. Despite this, the original concept of cooling by vapor compression, invented by John Gorrie, is still the most commonly used. As part of the constant search for newer technology in the world of science, we wish to examine

useful alternatives to the standard vapor-compression process. Therefore, it is the aim of this project to search for, analyze, and create a working model of an alternate refrigeration process.

BACKGROUND

Refrigeration has become an essential part of the way we live our life. Almost everyone has a household refrigerator, but not many know of the process required to produce the drop in temperature that we know as refrigeration. Nature works much like a heat engine, heat flows from high temperature elements to low temperature elements. As it does this, work is also done to its environment. Refrigeration is a process to keep a cool element cool or to reduce the temperature of one element below that of the other. The refrigeration process is, in essence then, a reverse heat engine; where heat is taken from a cold element to be transferred to a warmer element, generally by adding work to the system. In a heat engine, work was done by the system; so in order to do the reverse; work must be done to the system. This work input is traditionally mechanical work, but it can also be driven by magnetism, lasers, acoustics, and other means.

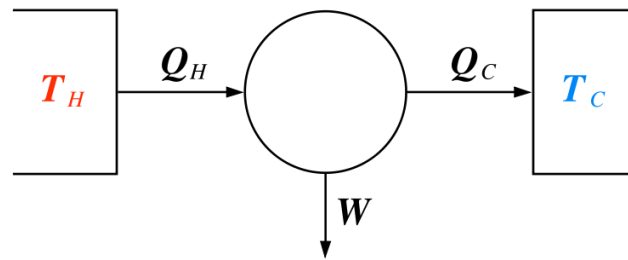


Figure 1 Heat engine thermodynamic schematic. (Karonen)

Several different types of refrigeration systems which utilize different work input were considered for this project. They are: the magnetocaloric refrigeration system, the thermoelectric refrigeration system, the vapor-compression system, and the absorption refrigeration system. A description of each system is given in the following section.

Refrigeration Cycles

Magnetocaloric Refrigeration System

The magnetocaloric refrigeration process uses magnetism as its work input to enable refrigeration. When solids, more specifically ferromagnets, are placed within a changing magnetic field, they experience an increase in temperature due to the reorganization of their molecular structure. The additional heat does not come from any external source, but is part of the internal energy of the solid. This behavior is known as the magnetocaloric effect (Vitalij K. Pecharsky, 1999). Figure 2 illustrates this effect on a gadolinium alloy.

In order to produce refrigeration using the magnetocaloric effect, a fluid, usually water or a solution mixture, is passed by the solid or Ferro magnet when it is in the magnetic field to absorb the irradiated heat from the solid. Once the heat has been absorbed, the solid is then removed from the magnetic field with less internal energy than it previously had; it experiences a drop in temperature when it restructures. The solid is, at this moment, colder than the desired compartment temperature and is used to drop the temperature of the compartment by natural heat flow. This is the generalized form of the magnetocaloric refrigeration system.

Magnetocaloric refrigeration systems are built using ferromagnets such as gadolinium or permanent magnetic plates that switch place in and out of the magnetic field to keep a constant heat flow. They utilize water or a mixture of water and ethanol as the heat transfer fluid, and use between 0.77 to 5 tesla of magnetic flux to induce the magnetocaloric effect. The lowest possible temperature attained with a magnetocaloric refrigerator is 38 K, with a cooling power of 600 Watts. The coefficient of performance for these systems ranges from 0.1 to 15 (Chubu Electric Power Co., 2006). These systems are not applicable for home use, however, due to the high magnetic field required to produce them.

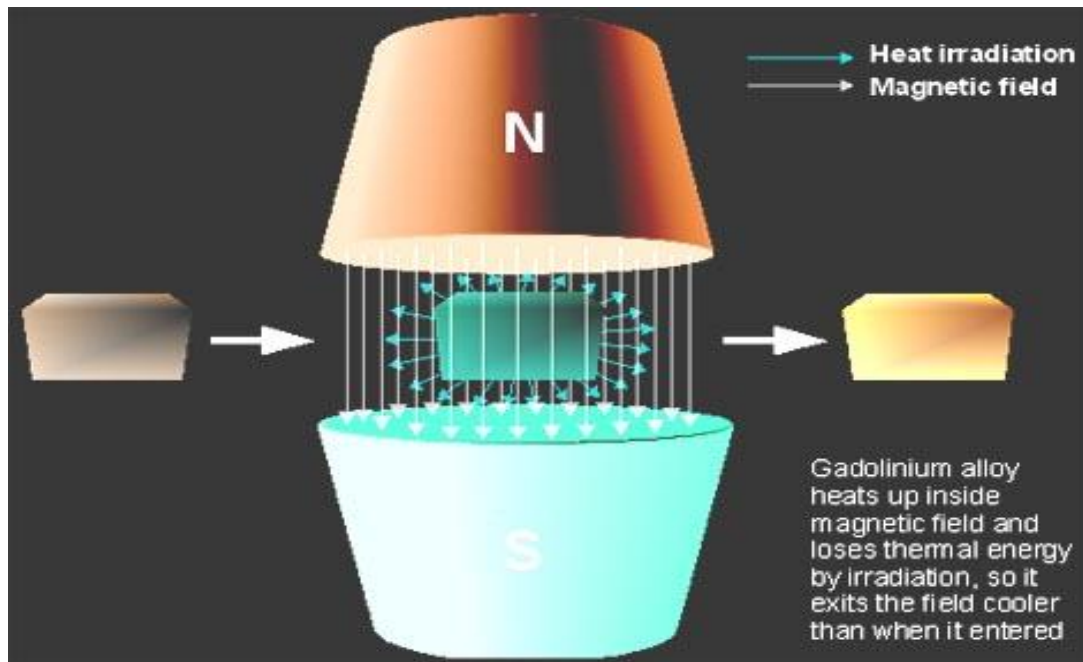


Figure 2 Magnetocaloric effect on Gadolinium alloy.

Thermoelectric Refrigeration System

When an electric current is passed through plates of different metals fused together, a heat flux is generated in the junction of the two plates. This phenomenon is known as the Petlier effect, and it is this effect that is used in a thermoelectric refrigeration system to produce cooling. A thermoelectric refrigerator comes equipped with only a thermoelectric plate, to facilitate the heat transfer, a fan, and fins to take the excess heat from the thermoelectric plate. Figure 3 is an illustration of a thermoelectric plate or module. Thermoelectric modules are constructed from a series of tiny metal cubes of dissimilar exotic metals which are physically bonded together and connected electrically. Solid-state thermoelectric modules are capable of transferring large quantities of heat when connected to a heat absorbing device on one side and a heat dissipating device on the other.

Because thermoelectric refrigeration units only require a thermoelectric plate, a fan, and fins, they can be made very small and are more lightweight than any other refrigeration system. Another advantage of thermoelectric refrigeration units is that they do not use any harmful refrigerants to facilitate refrigeration, which makes them environmentally friendly and safe. Thermoelectric refrigeration units do not wear out or deteriorate with use making them more applicable for military and aerospace purposes. Thermoelectric modules can also be reversed and be used for heating instead of cooling (koolatron).

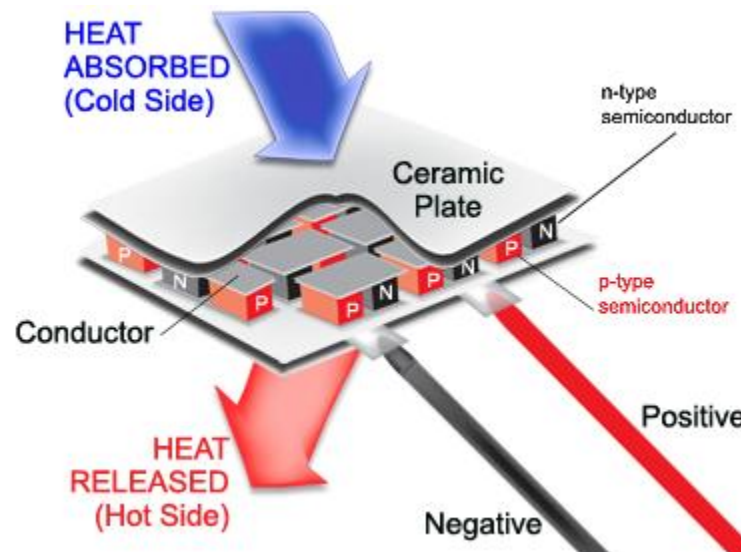


Figure 3 Thermoelectric plate diagram

The Vapor-Compression Refrigeration System

The vapor-compression refrigeration cycle is the most popular refrigeration cycle in use today. It has become a very important part of daily life, and can be found in everything from building and car air conditioning systems to refrigerators and freezers. This popularity is due to the fact that the cycle is relatively efficient, inexpensive, and compact.

A vapor-compression system is made up of four major components: a compressor, condenser, thermal expansion valve, and an evaporator. A liquid refrigerant circulates through the system, absorbing and releasing heat. The refrigerant enters the compressor as a saturated vapor as shown at point (1) in figure 4. As the refrigerant is compressed it increases in temperature and leaves the compressor as a superheated vapor. The superheated vapor enters the condenser, as seen in point (2), which is generally a coiled or finned tube cooled by air or water. At this point the refrigerant releases heat to the surroundings through convection and changes phase from a superheated vapor to a saturated liquid as the refrigerant cools to below its saturation temperature. The liquid is then funneled through the expansion valve, as indicated by point (3), where the sudden drop in pressure causes flash evaporation of the saturated liquid to a saturated vapor resulting in a temperature drop of the refrigerant which occurs because the drop in pressure across the expansion valve simultaneously lowers the refrigerant's saturation temperature. This change in temperature corresponds to the enthalpy of vaporization of the given refrigerant. The refrigerant only partially evaporates because the cooling produced from initial evaporation lowers the refrigerant temperature back to below its saturation temperature. The cold liquid-vapor mixture continues on to the evaporator, point (4), where it absorbs heat and fully vaporizes. This is the final stage, which accounts for the cooling in the refrigeration cycle. The vapor then enters the compressor, completing the cycle.

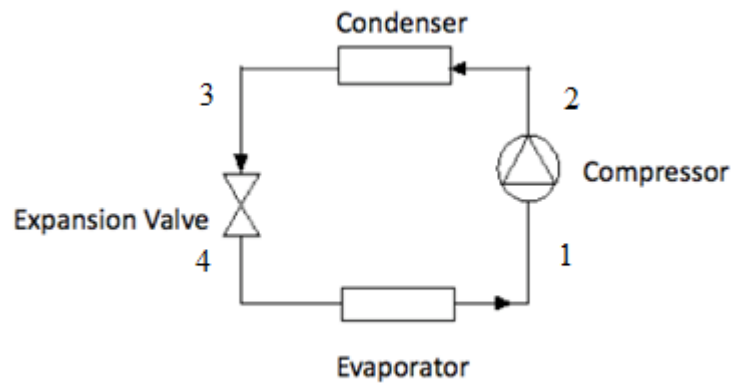


Figure 4 Vapor-compression system diagram

Vapor-compression refrigeration is so widely used because of its many advantages over other cycles. Common household cycles run at efficiencies of roughly 50% of Carnot's theoretical limit, which is about five times more efficient than its successor, the absorption refrigeration cycle (Jernqvist, 1993). Because a small amount of refrigerant liquid can produce a large amount of cooling, the system can be compact and still be efficient. This allows it to be both space saving and inexpensive.

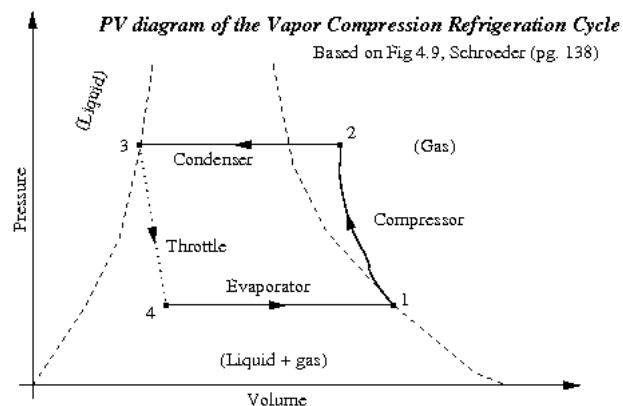


Figure 5 Vapor-compression P vs. v diagram

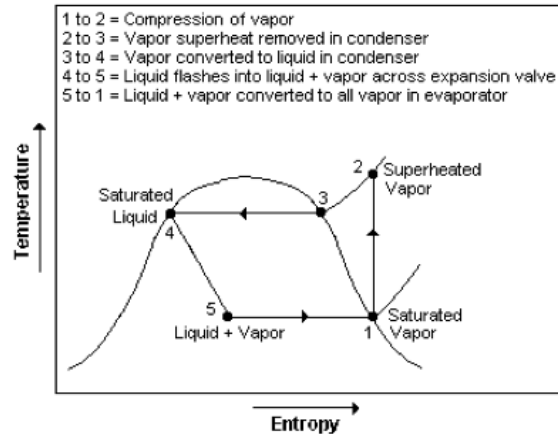


Figure 6 Vapor-compression T vs. s diagram

Despite all of the advantages, the vapor-compression refrigeration process still has few disadvantages. Many of the vapor-compression systems use hydro chlorofluorocarbon (HCFC) refrigerants. These refrigerants contribute to the depletion of the o-zone layer. Most systems that don't use HCFC refrigerants use hydro fluorocarbon (HFC) refrigerants. HFCs contribute to global warming and are generally less efficient (Devotta S.A.V, 2001). Another disadvantage of the vapor-compression systems is its dependency on electrical power. The vapor-compression systems must always be plugged in to a power source. This creates the need for them to be operated near an available electrical power source. The thermoelectric and some absorption refrigeration systems do not have this constraint.

The Absorption Refrigeration System

Unlike vapor-compression systems, absorption refrigeration systems use a heat source instead of electricity to provide the energy needed to produce cooling. Two major types of absorption refrigeration system design exist: the two fluid and the three fluid absorption system. The majority of both designs are generally the same; the differences between them lie in the way the liquid refrigerant is caused to evaporate. In a two fluid system, an expansion valve is used to

cause a large pressure drop, which causes the liquid refrigerant to evaporate. A three fluid system uses a third fluid to facilitate the expansion by means of partial pressures. The key processes in an absorption refrigeration system are the absorption and desorption of the refrigerant. A simple absorption system has five main components: the generator, the condenser, the evaporator, the absorber, and the solution heat exchanger. The flow of the refrigerant is through each of these parts in the different kinds of absorption system is given in each section. Figure 6 shows an absorption system that contains more stages for increased efficiency, but it still contains the five main parts.

Two Fluid Absorption Refrigeration System

Two fluid absorption systems are most commonly used in large buildings or plants where there is a significant source of waste heat available. In this section we will use the ammonia-water absorption refrigeration system example found in the *1997 Ashrae Fundamentals Handbook* to fully understand the workings of a two fluid absorption refrigeration system. This system is an ammonia-water refrigeration cycle system that is composed of an evaporator, a refrigerant heat exchanger, an absorber, a pump, two flow restrictors (expansion valves), a solution heat exchanger, a generator, a rectifier, and a condenser. Figure 7 shows the placement of each machine in the cycle, and the direction of flow of the solution mixture and ammonia vapor.

The cycle can be broken into different flows, one comprising of the ammonia-water mixture and the other comprising of the ammonia vapor alone. Points (1-6) are the cycle of the ammonium hydroxide solution, and the rest of the points constitute the ammonia vapor cycle. The solution rich in refrigerant at point (1) is pumped to higher pressure through the solution heat exchanger (2) into the generator (3) where heat is added and an ammonia-water vapor mixture is sent to the rectifier (13), and the solution poor refrigerant (4) is sent back through the

solution heat exchanger to the absorber. The ammonia-water vapor is purified in the rectifier by condensing the water vapor in the mixture into liquid. The pure ammonia vapor is sent to the condenser (7) and the water liquid is sent back to the generator (14). The ammonia vapor loses heat to the surrounding by convection as it goes through the condenser and is cooled into liquid ammonia (8). The ammonia liquid is passed through the refrigerant heat exchanger (9) for further cooling, and then passed through a flow restrictor (10) where it experiences a sudden drop in pressure and evaporates because this new pressure is less than its saturation pressure. The ammonia is now a saturated vapor at a temperature that corresponds to this new pressure. This temperature is always lower than the desired compartment temperature. The saturated ammonia vapor is sent to the evaporator where heat from the refrigerator is absorbed. The ammonia vapor (11) goes through the heat exchanger once again, but this time to absorb heat, before returning to the absorber (12) where it is absorbed into the water and the process repeats again. The mathematics used in obtaining the solutions in Table 10 for the five main components of an absorption system can be found in the system analysis and design section of this report.

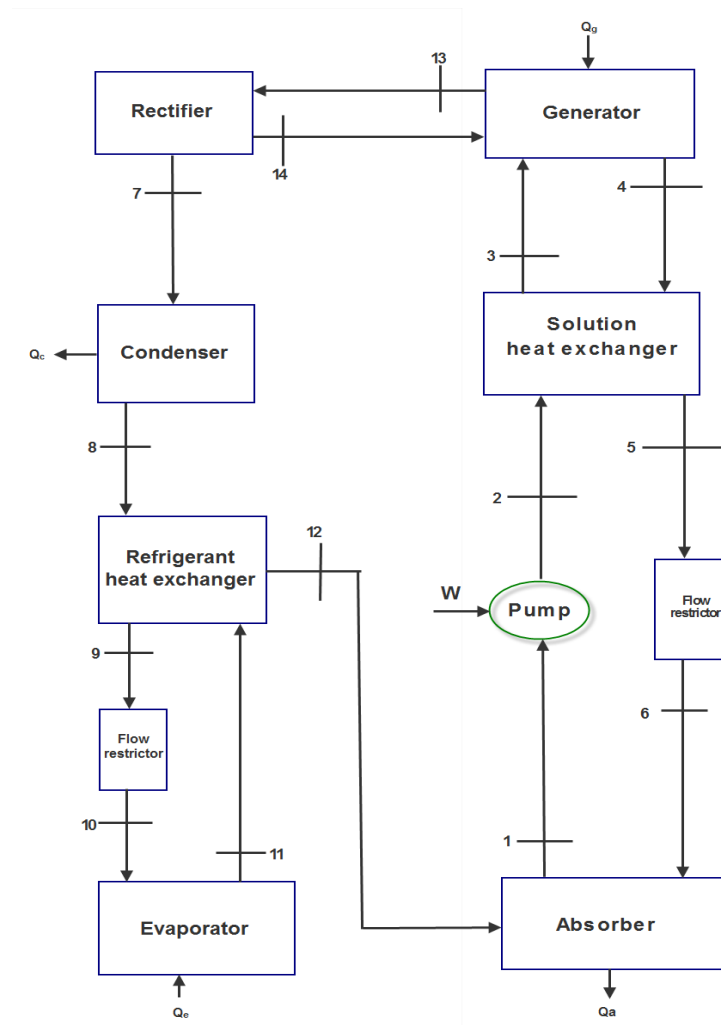


Figure 7 Ammonia-water single stage absorption refrigeration system flow diagram

The following tables were obtained from the Ashrae Handbook.

Table 9 Inputs and Assumptions for Single-Effect Ammonia/Water Model of Figure 7		
Inputs		
Capacity	$\dot{Q}_{\cdot e}$	1760 kW
High side pressure	p_{high}	1461 kPa
Low side pressure	p_{low}	515 kPa
Absorber exit temperature	t_1	40.6°C
Generator exit temperature	t_4	95°C
Rectifier vapor exit temperature	t_7	55°C
Solution heat exchanger eff.	$eshx$	0.692
Refrigerant heat exchanger eff.	$erhx$	0.629
Assumptions		
Steady state		
No pressure changes except through the flow restrictors and the pump		
States at points 1, 4, 8, 11, and 14 are saturated liquid		
States at point 12 and 13 are saturated vapor		
Flow restrictors are adiabatic		
Pump is isentropic		
No jacket heat losses		
No liquid carryover from evaporator to absorber		
Vapor leaving the generator is at the equilibrium temperature of the entering solution stream		

Table 10 State Point Data for Single-Effect Ammonia/Water Cycle of Figure 7						
No.	h_{sp} kJ/kg	\dot{m} kg/s	p kPa	Q Fraction	T °C	x , Fraction NH ₃
1	-57.2	10.65	515.0	0.0	40.56	0.50094
2	-56.0	10.65	1461		40.84	0.50094
3	89.6	10.65	1461		72.81	0.50094
4	195.1	9.09	1461	0.006	55.55	0.41612
5	24.6	9.09	1461		57.52	0.41612
6	24.6	9.09	515.0	0.006	55.55	0.41612
7	1349	1.55	1461	1.000	55.00	0.99809
8	178.3	1.55	1461	0.0	37.82	0.99809
9	82.1	1.55	1461		17.80	0.99809
10	82.1	1.55	515.0	0.049	5.06	0.99809
11	1216	1.55	515.0	0.953	6.00	0.99809
12	1313	1.55	515.0	1.000	30.57	0.99809
13	1429	1.59	1461	1.000	79.15	0.98708
14	120.4	0.04	1461	0.0	79.15	0.50094
COP _c = 0.571 ε = 0.692			W = 12.4 kW			

Using data from table 10, we were able to construct temperature vs. entropy diagrams that follows.

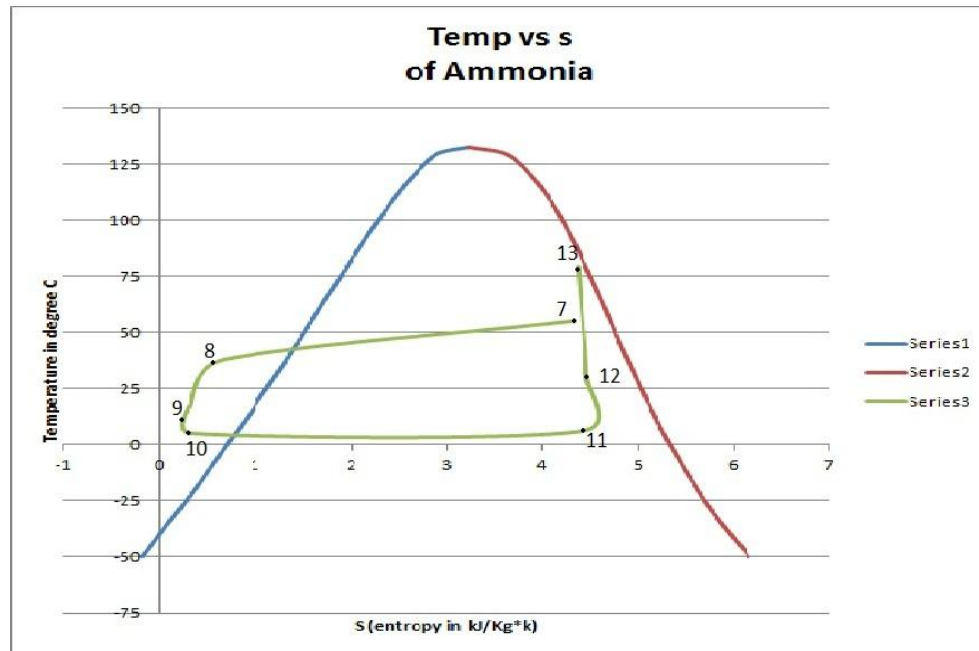


Figure 8 T vs. s graph of pure ammonia made from data in table 10.

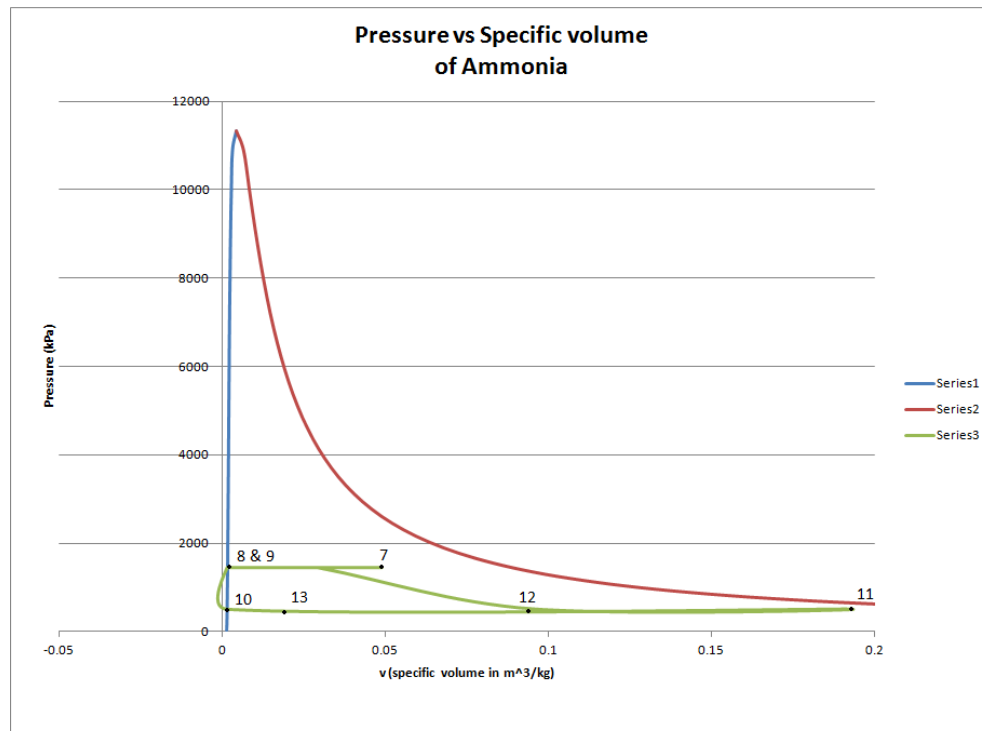


Figure 9 P vs. v of pure ammonia constructed from data in table 10.

From these graphs, particularly the T vs. s graph, we gain a further understanding of what happens to the ammonia gas in the system. It also illustrates the possible assumptions that can be made when doing an ideal analysis of the system. The T vs. s diagram in Figure 8 shows that the changes happening from points 9-10 and that of points 11-12 are nearly isentropic, meaning that there is no change in entropy. Entropy is a measure of heat energy per unit of temperature that is lost or gained during a process which is not used for work. When doing a thermodynamic analysis of the system, these changes can be assumed to be isentropic without substantial errors occurring. It is also interesting to note that points 12 and 7 are also nearly isentropic; therefore, the ammonia-water mixture cycle can be simply understood as a step of processes to return the ammonia entropy to its original value at point (7) and may be substituted by a simplified model that accomplishes the same end. The T vs. s diagram also clarifies that there is, in fact, no temperature change in the ammonia vapor as it goes through the evaporator. On the P vs. v diagram of Figure 9, one can see those processes that are isobaric, meaning that no change in pressure takes place. One can also see the effect of the heat exchanger in the density changes from points (11) and (12).

Absorption refrigeration cycles often have a very low coefficient of performance. Ashrae tells us that single-effect absorption refrigeration systems have a peak cooling COP of around 0.7, but this performance can be augmented if the system is redesigned with some additional parts to use the rejected heat of the system. Their performance can be increased to a range of 1.0-1.2 depending on the design and application. This fact illustrates that the usefulness of an absorption refrigeration system comes from the utilization of excess heat from any system, even its own.

Three Fluid Absorption Refrigeration System

The refrigerator built for this project is a gas absorption refrigeration system that uses three fluids instead of the typical two fluids. Of the various refrigeration cycles, the three fluid absorption system is the only one that does not require electricity or mechanical parts to operate. It is run entirely by heat. The key to its use is the third fluid, used to regulate the partial pressure of the refrigerant, and therefore, its saturation temperature. A low partial pressure of the refrigerant allows the refrigerant's saturation temperature to decrease and create cooling. The system remains at constant total pressure and eliminates the use of expansion valves. Most three fluid absorption systems use ammonia as their refrigerant and hydrogen as the 3rd fluid. A generic diagram of a three fluid absorption refrigeration system that uses ammonia and hydrogen is shown in Figure 10. Beginning with point 1 the seven stations have the following characteristics: at (1) the application of heat vaporizes the strong ammonia-water solution up into the bubble pump. At (2) the solution and gas passes into the separator where the water vapor condenses to liquid and passes through a separate series of tubes back to the absorber. Superheated ammonia vapor now rises to the condenser, leaving a small amount of weak ammonia-water solution pooled in the separator. At (3) the ammonia is traveling through the condenser, releasing heat to the surroundings and condensing back to a liquid state. At (4) liquid ammonia meets with hydrogen and enters the evaporator. Here, the partial pressures of the hydrogen and ammonia lower the saturation temperature of the liquid ammonia, causing the ammonia to evaporate. This expansion lowers the temperature of the hydrogen-ammonia mixture, allowing it to absorb heat from the refrigerator compartment, which provides cooling. At (4a) the hydrogen-ammonia mixture exits the evaporator into the absorber in a gaseous state. In the absorber the gaseous ammonia and hydrogen meet with liquid water. The ammonia is less dense than hydrogen, causing it to sink and consequently accumulate under the hydrogen.

This increases its partial pressure and induces a phase change back to liquid. Ammonia and water are capable of forming a solution together as ammonia is soluble in water. Hydrogen is incapable of mixing and continues to circulate back to the top of the evaporator as a pure gaseous substance. The ammonia and water solution exit the absorber and travel to the generator. It then begins the cycle again.

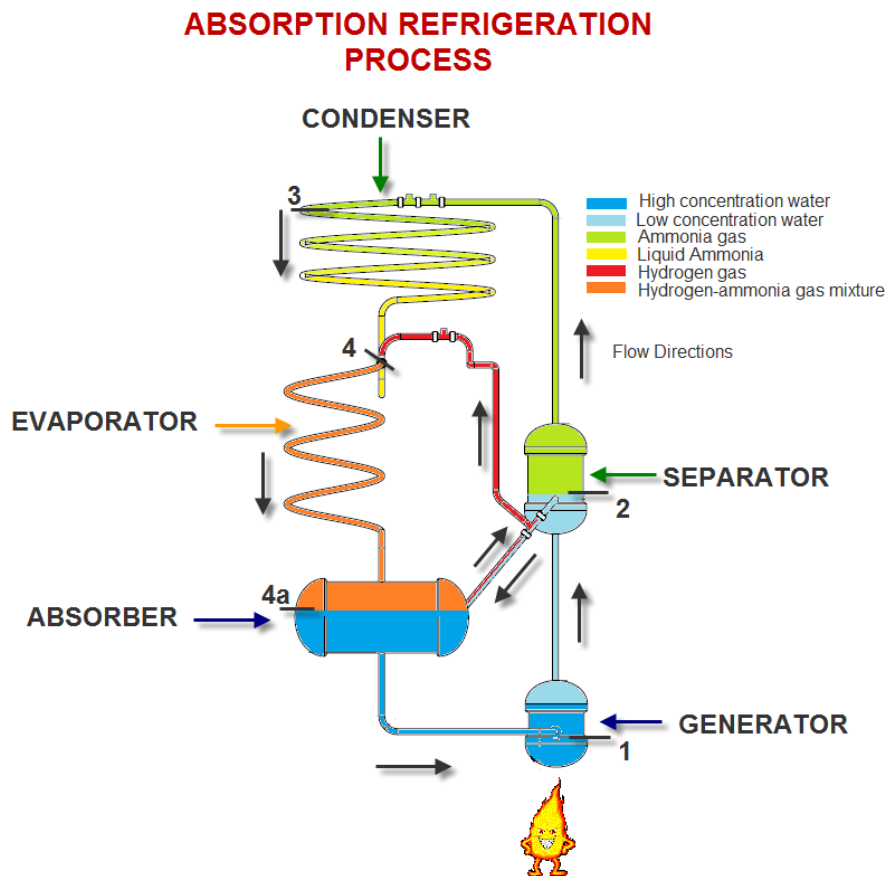


Figure 10 Diagram with state points of a basic three fluid absorption system.

The novelty of this cycle is the lack of moving parts and electricity to drive them. This creates a very independent unit that can continue to run indefinitely so long as it is provided heat. The disadvantage is a low thermal efficiency relative to common refrigeration. A tremendous

amount of heat required to separate water and ammonia relative to the heat drawn in from the refrigerator.

System Selection

This project will focus on the design and fabrication of a three fluid gas absorption refrigerator. This choice was made to investigate alternate forms of refrigeration. The thermoelectric refrigerator, perhaps with the exception of the plate, is simple; and the magnetic refrigerator is very complex and may not be done in the time allotted for this project, and it also requires a large magnetic field (about 1.5 tesla (Organization, 2006)) in order to operate. A three fluid gas absorption system, physically, is simple, containing only tanks and pipes. This would make it much more likely to fit into our budget and have less construction complications. Therefore, a three fluid gas absorption refrigerator was chosen.

SYSTEM ANALYSIS AND DESIGN

The system is a three fluid absorption refrigeration system designed to operate under an ambient temperature of 20°C while cooling the inside compartment to 3°C. We begin our analysis with the refrigeration compartment.

Refrigerant and Third Fluid

In a three fluid absorption refrigerator, the refrigerant comes into direct contact with the third fluid in the evaporator and must be separated from it in the absorber. Water is the medium used to facilitate the separation of the refrigerant from the third fluid, so the choice of refrigerant must be minimally or non-reactive to the third fluid and highly soluble in water. The third fluid must, on the other hand, be virtually insoluble in water.

Aside from the aforementioned requirements, the refrigerant must also meet standard refrigerant characteristics listed below. A refrigerant must be or have

- ozone and environmentally friendly
- low boiling temperature
- vaporization pressure lower than atmospheric
- high heat of vaporization
- nonflammable and non-explosive

Most manufacturers use ammonia as a refrigerant because it has a greater heat of vaporization, a lower vaporization pressure, a higher auto-ignition temperature, and is 100th time more soluble in water than other refrigerants. Ammonia was, therefore, chosen as the refrigerant for this project.

Two non-reactive and insoluble gases considered for use as the third fluid were hydrogen and helium gas. In the consideration of the third gas, the only requirement is that the fluid be insoluble in water which both these gases meet with negligible differences. The difference in refrigerator performance obtained between these two gases lies in the rate of absorption of the refrigerant in water or the absorbent due to buoyancy effects. This can be understood by looking at a simplified model of the absorber shown in figure 11. A gas mixture of soluble gas A and insoluble gas B is flowing down a rectangular tube towards a liquid C. At some distance L from the liquid surface, gas B has a mole fraction of x_{B1} some distance L above the liquid interface and at the liquid surface it has a mole fraction of x_{B2} . The two side walls are impermeable.

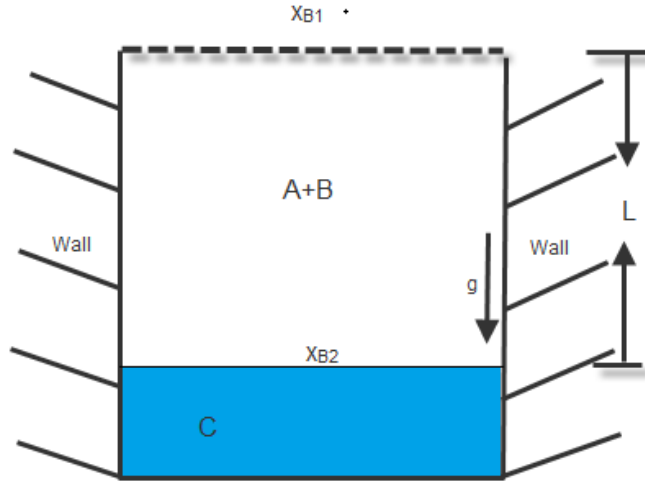


Figure 11 simplified model of absorber.

X_{B1} = mass fraction of B some distance L above the liquid interface

X_{B2} = mass fraction of B at the liquid interface

Because gas A is absorbed into liquid C, we know $X_{B2} > X_{B1}$. Since the density of gas B (hydrogen) is much smaller than that of gas A (ammonia), the vapor mixture at B2 is lighter than the mixture at B1. This will induce convection inside the enclosure do to buoyancy, and it is this convection that causes a performance difference between hydrogen and helium. There are no direct mathematical methods to calculate convection cells, but experimental analysis does yield a mathematical formula using Sherwood number.

$$Sh = 0.069 * \frac{1}{x_{B2}} * Ra_m^{\frac{1}{3}} * Sc^{0.074}$$

$$Sh = \text{sherwood number} = \frac{\text{convective mass transfer coefficient}}{\text{Diffusive mass transfer coefficient}} \quad [3]$$

$$3E5 < Ra_m < 7E9$$

$$0.02 < Sc < 8750$$

Ra = rayleigh number

$Sc = \text{schmidt number}$

This equation was applied to hydrogen and helium using experimental data ($Sc = 0.957, 1.01$ and $Ra_m = 2.04E6, 1.58E6$ for hydrogen and helium, respectively), and it was found that the Sherwood number of hydrogen was 9% greater than that for helium for the buoyancy induced convection configuration (chen & Herold, 1995). It was, therefore, chosen that hydrogen gas is to be used as the third fluid for this project.

Having now selected the refrigerant of choice, the total system pressure can now be obtained because it is dependent on the type of the refrigerant used. Before entering the evaporator, pure ammonia refrigerant leaves the condenser in a liquid phase at the ambient temperature of 20 °C. The saturation pressure of ammonia at ambient temperature must, therefore, be the overall system pressure. At 20 °C the saturation pressure of ammonia is 9.00 bar; but to ensure that the refrigerator works for a range of temperatures it was decided to have the operating pressure at 10 bar instead. This would allow the ammonia to liquefy at 24.89 °C. After the flash vaporization of liquid ammonia, it was arbitrarily chosen that the difference in temperature between the cabinet compartment and the ammonia fluid that would facilitate heat transfer is 8 °C. This means that since the cabinet has a temperature of 3 °C, the vaporized ammonia gas should have a pressure that corresponds to a temperature of -5 °C. At this temperature, the saturation pressure of ammonia is approximately 3.5 bar. In order to drop the ammonia pressure to 3.5 bar to facilitate vaporization, the third fluid is used in a mixture with the ammonia. Using Dalton's Law of partial pressure, which states that the overall pressure of a mixture is the sum of the partial pressure of each of the gases in the mixture. We can find the required third fluid or hydrogen pressure needed in the mixture to lower the pressure of ammonia to 3.5 bar.

$$P_T = P_{H_2} + P_{NH_3} \quad [4]$$

Where $P_T = 10.00$ bar, and $P_{NH_3} = 3.5$ bar.

$P_{H_2} = 10.00 - 3.5 = 6.5$ bar of H_2 gas is required in the evaporator mixture.

Material Selection

The most important aspect of the material selection process was the selection of a material that could withstand the corrosive effects of ammonia, both in its liquid and its gaseous form. Also, the material had to be able to withstand the system pressure of 160 psi while under a temperature load of 200 °C and still be malleable enough to be bent into whatever shape was required. After consulting with Professor Sisson, Director of the WPI Materials Science Program, we found that the metal most suited to our need and specifications was the 300 series stainless steel metal. Stainless steel parts are much more expensive than others, however. After compiling an initial cost sheet of all stainless steel materials, we realized that stainless steel was much too expensive. An alternate to stainless steel is carbon steel. Carbon steel is less costly than stainless steel, it is not corroded by hydrogen gas, and its corrosion rate against ammonia hydroxide is acceptable for temperatures less than 300°C (Uhlig, 1948). Since we do not expect to have a temperature greater than 150°C, carbon steel was the material of choice for this project. Other materials such as glass and some plastics do possess a corrosive resistance to ammonia, but there were none we could find that could resist both the high temperatures and pressures of our system.

Refrigerator Cabinet

The purpose of a refrigerator cabinet is to allow as little heat transfer from the surroundings to the inside of the cabinet. In other words, it is to keep the inside of the cabinet as insulated as possible so that the refrigerator system does not have to do as much work. In its simplest form, a cabinet is an insulated volume. The amount of heat transferred to the cabinet dictates the amount of work a refrigerator will need to do and this in turn affects the size of the parts of the whole refrigerator. Heat is transferred through convection, conduction, and radiation; but radiation can typically be neglected. It is, therefore, important to choose an insulation material with a low conduction coefficient. For this project, the insulation of choice was chosen to be Styrofoam because of its ease of use, availability, cost, and low conduction coefficient. The size of the refrigeration compartment was dictated only by the basis of what was thought to be a reasonable size for a small demonstration unit. The most critical thing to understand is that the heat flow into the refrigerator will dictate the sizes and values of the components of the remainder of the system. Thus sometimes a process of guess and check becomes necessary until solutions are found which are adequate. This will be explained below.

Our design process was as follows. Initially we arbitrarily selected an external compartment size of 8inx8inx6in inches, again this was chosen based purely on what we thought would be reasonable for our purposes. We then set out to model the heat flow into the compartment. The following two equations were used to model the heat transfer into the refrigerator compartment:

$$Q = \frac{T_{\infty} - T_r}{R_{tot}}$$

$$R_{tot} = \frac{1}{h_1 * A} + \frac{t_w}{K * A} + \frac{1}{h_2 * A}$$

$A = \text{surface area}$

$h_1 = \text{convection coefficient rate between air and outer surface}$

$h_2 = \text{convection coefficient between the inner walls and inside air}$

$K = \text{conduction coefficient}$

$Q = \text{heat transfer}$

$t_w = \text{wall thickness}$

$T_\infty = \text{ambient temperature of the air}$

$T_r = \text{temperature of refrigerator compartment}$

These equations set up a circuit of heat resistance, analogous to an electrical circuit, through the wall of the refrigerator. The heat transfer resistance rates are taken in series like resistors in an electric circuit with the change in temperatures being equivalent to the voltage change and the heat transfer equivalent to the current flow.

$$I = \frac{V}{R}$$

$$Q = \frac{T_\infty - T_r}{R_{tot}}$$

Our circuit consists of the three resistances to heat flow listed previously; $h_1 A$ between ambient air and outer surface, t_w / KA through the box wall, $h_2 A$ between inner wall and inner air.

Next, to properly analyze the refrigerator compartment required a simultaneous analysis of the approximate length of the internal piping needed. For example, say we chose a 1" thickness and guessed h_1 and h_2 coefficients and analyzed the heat flow through all sides. We then later analyze the proper piping length in our compartment and find out that it is too large to

fit. We would then have to go back and adjust thicknesses of the compartment wall until we found a satisfactory size for the pipe. To avoid this problem of being forced to return and modify compartment numbers later, we modeled to evaporator pipe length simultaneously.

At steady state, with a chosen refrigerator air temperature of 3°C, the heat transfer into the refrigerator must equal that into the evaporator pipe and therefore liquid ammonia by heat flow conservation. Thus our Q value for thermodynamic energy balance is the same as that for the refrigerator. Our thermodynamic energy balance is:

$$Q - W = \dot{m}_2 * \left(h_{2sp} + \frac{v_2^2}{2} + g * Z_2 \right) - \dot{m}_1 * \left(h_{1sp} + \frac{v_1^2}{2} + g * Z_1 \right)$$

In a flowing fluid there is no work except that of pressure which is included in the enthalpy term, velocity is so low it is insignificant, and potential energy change is small compared to that of enthalpy and therefore neglected. So our 1st Law of Thermodynamics reduces to:

$$Q = \dot{m} * \Delta h_{sp}$$

Where \dot{m} is mass flow and Δh_{sp} is enthalpy change.

As stated our heat transfer rates everywhere must be equal at steady state. So using the approximation of a thin walled pipe we neglect the conduction rate through the pipe. For a system with two fluids at different temperatures separated by a pipe wall, we have the following general equation that we can use to model:

$$Q = U * A * \Delta T_{lm}$$

The first term U is the effective convection coefficient between the two fluids. The third is the logarithmic mean temperature. This gives us the average difference in temperature

between the two fluids. Q will change with ΔT , and as ΔT approaches zero the heat transfer rate and time to equilibrium goes to infinity. Because of this time increase, the true representative mean temperature is closer to the final ΔT than the initial. Knowledge of the log mean temperature allows us to evaluate Q , and ultimately area, more accurately.

The term U is similar to the resistance. It is an effective coefficient between the two fluids. It is essentially the same as R_{tot} but its inverse. It is defined as:

$$U = \frac{1}{R_{tot} * A}$$

Therefore in equation form it is:

$$U = \frac{1}{\frac{1}{h_1} + \frac{1}{h_2}}$$

This is the same form as that of the effective spring constant k for two springs in series with each other. The result is that the effective constant, in both cases, is lower than the lower of the two. To ensure an accurate analysis of pipe length we must determine h_2 properly. h_1 is typically about $5W/m^2 K$ for ambient air, and will not be calculated here, but h_2 is very much dependent on the internal flow conditions. For single phase laminar flow h_2 could be very low, possibly lower than h_1 . But, in our system the great majority of the heat transfer occurs in two phase flow. So, our lengths will be determined largely by this flow regime. One formulation we have encountered for two phase flow convection is:

$$h = 0.555 * \left(\frac{g * (p_l) * (p_l - p_g) * k_l^3 * (h'_{fg})}{\mu_l * (T_{sat} - T_s) * D} \right)^{1/4}$$

Where, p_l and p_g are liquid and gas density, k_l^3 is liquid conduction coefficient, h'_{fg} is modified latent heat which is given as a separate equation, μ_l is coefficient of liquid viscosity, T_{sat} is flow

temperature, and T_s is wall temperature. We won't go through all the numbers here but our calculation for evaporator two-phase flow coefficient came out to be $h_2=4,868.696\text{W/m}^2 \text{ K}$. Essentially what this tells us is that in the two phase region fluids very readily absorb heat. So our U will be limited primarily by ambient air convection. Looking at the U equation, with such a large h_2 the h_1 term will dominate and U will be approximately equal to h_1 . So, in the following analysis we will use $U=h_1=5\text{W/m}^2 \text{ K}$ to model heat transfer.

One further simplification we make to the equation for Q given previously is in the log mean temperature term. As will be shown, most of our heat transfer occurs in the two-phase region which is at constant temperature. So our ΔT will be constant; there is no need to compute log mean temperature in our case. Making these simplifications our heat transfer equation simplifies to:

$$Q = h_1 * A * (T_r - T_s)$$

T_r = refrigeration temperature

T_s = pipe external temp, taken as equal to the fluid temperature

Rearranging to solve for length we get:

$$L = \frac{Q}{\pi * D * h_1 * (T_r - T_s)} = \frac{\dot{m} * \Delta h_{sp}}{\pi * D * h_1 * (T_r - T_s)}$$

Using this equation for L , we can relate pipe length directly to heat transfer into the refrigerator or mass flow and enthalpy if we wish. This equation will be used in detail in the following evaporator section.

Now, with our equations established we began our analysis. We proceeded through a trial and error process of varying Styrofoam wall thicknesses and box dimensions to obtain a practical evaporator length. The original dimensions of 8inx8inx6in at 1inch thickness produced

a length of less than 1m, but we nevertheless decided that it was simply too small for our purposes and tried altering the box dimensions to 8inx8inx6in internally with 1inch wall thickness. But this meant too much pipe length increase even for the new dimensions. For example if we increased the dimensions of all sides by 1in from 7inx7inx5in to 8inx8inx6in, the area of the larger sides would be 49in^2 and 63in^2 respectively. This is a 23.438% increase in area for a 12.5% dimension increase. This means a roughly a 23% Q increase and 23% length increase. The point being that pipe length increases at a greater rate than dimensions. So this necessitated adding more outer insulation. As seen from the equation of R_{tot} , increasing t_w with all parameters remaining fixed will roughly linearly decrease heat transfer and pipe length. This is because the conduction term is far larger than the two convection terms due to the value of K. So by trial and error we found a combination that produced adequate size and small enough pipe length to fit within the box. We ended up settling on 2inch refrigerator wall thickness, and interior dimensions of 8inx8inx6in. We found that we needed to completely insulate two 6inx8in sides of the box to provide low enough heat transfer without increasing wall thickness to about 5inches. The numbers and result used are listed here:

$$h_1 = 10 \frac{\text{W}}{\text{m}^2\text{K}} \quad h_2 = 8 \frac{\text{W}}{\text{m}^2\text{K}}$$

$$t_w = 2'' = .0508\text{m} \quad K = .03975 \text{ W/m}$$

$$A_{6 \times 8} = .03097\text{m}^2 \quad A_{8 \times 8} = .04129 \text{ m}^2$$

$$R_{\text{tot}6 \times 8} = 48.532 \text{ K/W} \quad R_{\text{tot}8 \times 8} = 36.3994 \text{ K/W}$$

$$Q_{\text{tot}} = 1.6345 \text{ Watts}$$

This produced a corresponding evaporator length of 1.3m, approximately. These results seemed reasonable and we decided to keep the heat input of 1.6345 watts, and thus the approximate evaporator length. But, the design of the refrigerator compartment did not end here.

Our original idea had been to buy sections of Styrofoam and to manually construct the box. But, we were able to find a Styrofoam box of reasonable size relative to what we wanted, with a reasonable thickness as well. Since cutting and gluing together Styrofoam can be a tricky process we decided to use this readily available box. At this stage of our work we had been using the previously given numbers for some time. Rather than reanalyzing the box and our numbers since, we decided to analyze the new box and add insulation such that we could maintain the previous net heat flow in at our operating condition of 3°C. Our new box had the dimensions of 7.625inx7.625inx10.69in with a wall thickness of 1.5in.

This time, we decided to conduct an exact analysis of the convection coefficients for the greatest accuracy. Previously we had taken guesses about the convection coefficients. We had not analyzed them exactly previously, as we assumed that air flow conditions around the compartment would change so frequently as people moved past it or perhaps as a heating or ventilation system turned on or off in the building that we could never determine them with any significant accuracy. This was still true, but now we needed to produce the heat flow required above of 1.6345 watts. This would require us to model it as accurately as possible even if it could never be 100% on target. We therefore began an exact analysis of the convection coefficients.

A natural convection coefficient is fundamentally determined by the orientation of the surface it is on and the temperature difference between the surface and ambient air. The type of

heat transfer is dependent upon this temperature difference. If the ΔT is too low than a stable temperature gradient will exist and heat transfer will occur by conduction. If ΔT exceeds a critical value then buoyant forces of the gases will be able to overcome viscous retarding forces, and air movement occurs. This is the fundamental parameter in finding h.

In typical convection we use empirical correlations for Nusselt number, $Nu=h*L/k$, to find h based on Reynolds and Prandtl number. For natural convection, which is driven only by ΔT , Nusselt number is based on a parameter called Grashof number. It is derived from boundary layer momentum and energy conservation. This is given by:

$$Gr_L = \frac{g * \beta * (T_s - T_\infty) * L^3}{\nu^2}$$

The term β represents the volumetric thermal expansion coefficient. It is a measure of the change in density with change in temperature. Thus it is a parameter for measuring viscous vs. buoyant characteristics. It is given by:

$$\beta = \frac{(\rho_\infty - \rho)}{\rho * (T - T_\infty)}$$

However, for ideal gases it can be simplified to:

$$\beta = \frac{1}{T}$$

Our final parameter is Rayleigh number. Rayleigh number is simply a number used to determine the type of convective flow, laminar or turbulent. It is the correlation commonly used in empirical correlations for natural convection.

$$Ra_L = Gr_L * Pr$$

The term P_r represents Prandtl number. Prandtl number is a measure of the ratio of thermal to viscous diffusivity of a substance. It partly determines how it responds to temperature gradients or momentum gradients.

We now decided to analyze the compartment with a horizontal orientation. That is, the long side of 10.69inches being horizontal. So our vertical height is then 7.625inches. To analyze Grashof number and the film temperature for finding β we must know the surface temperature of the box.

We could find this by newtons law of cooling:

$$Q = h * A * (T_{\infty} - T_{s1})$$

$$T_{s1} = T_{\infty} - \frac{Q}{h * A}$$

Where T_{s1} is the outer surface temperature of the box. To find T_{s1} we must guess an h value. We also do not know Q , in this exact analysis Q will change through each side depending on it's orientation. To obtain Q we reuse our original resistance equations:

$$Q = \frac{T_{\infty} - T_r}{R_{tot}}$$

$$R_{tot} = \frac{1}{h_1 * A} + \frac{t_w}{k * A} + \frac{1}{h_2 * A}$$

We know the internal temperature and ambient, so to find R_{tot} , we must guess a value of h_2 as well. Doing so we obtain total resistance and Q through the particular side. We then can find T_{s1} . With our temperatures now known we can evaluate all fluid properties, and β , Grashof

number, Rayleigh number, and Prandtl number. For a vertically oriented plate we then used the following empirical correlation:

$$Nu_L = \left(0.825 + \frac{0.387 * Ra_L^{\frac{1}{6}}}{\left(1 + \left(\frac{0.492}{Pr} \right)^{\frac{9}{16}} \right)^{\frac{8}{27}}} \right)^2 = \frac{h * L}{k}$$

There are additional correlations that we used as well. These are for a horizontal plate facing upward, and a horizontal plate facing downward.

The process for solving for every exterior side consisted of the following. Guessing an h_1 and h_2 to find Q , and then T_{s1} . Then solving for all properties and numbers and ultimately for h_1 . Then, assuming our guess of h_1 was far enough off, we must reguess h_1 and resolve for Q , T_{s1} , and ultimately h_1 again. When finally the solutions converge we must then go about finding h_2 within the box. It might seem that we could stop after finding h_1 as we would know Q at this point which is primarily what we need, but we can't forget that h_2 will affect the ΔT across the wall which will alter the surface temperatures and h_1 results, as well as changing the total resistance and heat flow. So, we must find h_2 as well. The process for doing so is much the same as before. We must guess an initial h_2 , then find Q , and T_{s2} , and ultimately after doing this several times by guess and check, get the actual h_2 . This is a tedious process that must be done for all the different side orientations of the box. To go through it here would require excessive length, and we present only the results of this process below.

Side dimensions and Orientation	$h_1 \left(\frac{W}{m^2K} \right)$	$h_2 \left(\frac{W}{m^2K} \right)$	$R_{tot} \left(\frac{K}{W} \right)$	Q (W)
7in x 10in side	3	2.6	31.8863	0.53
7in x 10in top	4.3	2.8	29.45	0.5773
7in x 10in bottom	3.9	5	26.912	0.63
7in x 7in side	2.95	2.8	44.112	0.3854

$$Q_{tot} = 2(Q_{(7x10)side}) + Q_{(7x10)top} + Q_{(7x10)bot} + 2(Q_{(7x7)side})$$

$$Q_{tot} = 3.0441W$$

We have used 7inx7in and 7inx10in above to describe the sides rather than the exact decimal number.

The resulting h values are, for the most, part fairly low. Typically they do not drop much below 5 in most applications. But, we had very small temperature differences between surface and ambient. Typically only about a degree kelvin or less. Without any forced flow, a single degree will produce very slow heat transfer. In addition the rayleigh numbers we used all fell within the accepted range for each correlation, corroborating that the results are valid even if not perfect. We stated that we wished to maintain 1.6345 watts of heat into the compartment. In order to do so, we need to completely insulate both 7.625inx7.625in sides and the 7.625inx10.69in bottom side. This will eliminate 1.401 watts of heat and leave us with 1.64 watts, almost exactly the amount we desire. It should be stated that the empirical correlations used typically have an error margin of +/- 5-10%. Adding in the fact that there can be significant

human error in any guess and check type process the numbers given are within range of their true value but should not be assumed to be exact.

Evaporator

All gas absorption refrigeration systems rely on evaporation of liquid ammonia into hydrogen to produce cooling. It is commonly stated that Dalton's law of partial pressure is what causes this to occur. We have so much hydrogen mass, and so much vapor ammonia mass such that a correct partial pressure is established. This partial pressure reduces the evaporation temperature of ammonia to below that of the refrigerator to allow it to evaporate. In truth Dalton's law of partial pressures does not play a role in the actual ammonia evaporation. It is only a secondary parameter. In any general fluid-gas system, the on the liquid, not accounting for depth pressure, is always at the pressure of the gas at its interface. So, the liquid ammonia which enters the evaporator will be at 10 bar of pressure, due to mostly hydrogen and a small quantity of ammonia gas, which returns from the absorber. At this pressure it will not evaporate until 24.89. So the question is then, what does cause it to evaporate?

The answer to this can be explained in psychometrics and mass diffusion. Starting with a simple example helps to explain it. A puddle on the side of the street has the same dilemma. It does not boil until 212°F, but yet throughout the course of the day it evaporates. The reason is that liquid and vapor phases always seek specific thermodynamic energy equilibrium with each other. When a liquid is at say 20°C it will have a corresponding saturation pressure call this pressure, P_n , as it will at any temperature. To be in specific energy equilibrium the liquid will want to have this vapor pressure (due to its own gas phase, not total gas pressure) P_n , existing in the gas above it. If say we have a jar consisting of liquid water with air above it at standard temperature and pressure the liquid water will continue to release vapor by drawing in heat from

the surroundings, or itself, until the air above it has a water pressure of P_n . The enthalpy necessary to perform this phase change is given by that two-phase state's properties. To provide another alternate example consider moisture condensing on a cold glass of water. The surface temperature of the glass is very low, say 3°C. But the air is at 20°C. At 20°C water vapor can constitute 0.02339 of atmosphere by pressure. But at 3°C near the glass it can only be about 0.0071 bar. This means that it has a much lower maximum humidity content and therefore must condense. The outside of the glass is then wetted.

Alternately we can explain it by Diffusion Mass Transfer, hence the reason three fluid gas absorption refrigerators are sometimes called diffusion absorption refrigerators. There are two fundamental principles we need to know here, some of this was presented in the third fluid analysis section previously. The first is that just as temperature difference is the driving force for heat transfer, mass concentration difference is the driving force for mass diffusion. If you had a partitioned box with 90% of gas A on one side, but only 15% gas A on the other side and removed the partition, the two gases would diffuse until reaching equal concentration everywhere. The second principle is that at the interface of a liquid with vapor, the conditions correspond to that of saturation. So, at the liquid interface its own vapor constitutes a pressure of that of saturation pressure, P_{sat} , for the given temperature. In the case of a liquid such as water, or ammonia in our case, when the above gas is lower in its own vapor pressure than P_{sat} mass diffusion will begin. The liquid will release vapor by drawing in heat until the concentration gradient above it is eliminated. In the case of a puddle of water, it never reaches a stable gradient as air flows over it throughout the day continuously causing evaporation. So, the principles of psychometrics and mass diffusion tell the same story from a different perspective. They verify for us that evaporation will occur even without two-phase equilibrium heating which

is the most common method. Note, we keep referring to water and air as it is a simple and common daily example. Ammonia and Hydrogen are analogous, the ideas presented in psychometrics and mass diffusion apply to any liquid-gas combination assuming they do not interact as water and ammonia do.

Before presenting a formal discussion of Ammonia and Hydrogen, it is useful first to discuss the Joule-Thomson effect. It assists in understanding the subsequent analysis. The Joule-Thomson process is a throttling process commonly used in expansion valves, and specifically in refrigerators. When we want to expand a condensed liquid to lower pressure and temperature before entering the evaporator of a standard refrigerator, we pass it through a partially blocked passage or a porous plug. Mechanical work becomes necessary to overcome this blockage and as a result pressure drops. With this drop, which is determined by the size of the plug relative to the passage, the fluid pressure falls below that of saturation. As a result the fluid will want to vaporize. But, the process is kept insulated so it is adiabatic. The only way for the fluid to vaporize is for it to provide its own energy of vaporization.

So just as the diffusion and psychometric evaporation draws heat from the surroundings, the Joule-Thomson expansion must draw heat from itself as it is insulated; the process is called isenthalpic meaning constant enthalpy. As a result its temperature drops, and the fluid partially vaporizes until temperature-pressure equilibrium is reached. This all occurs so suddenly that this is often also called flash vaporization. As a result the evaporation formally begins in the two-phase region with a certain quality rather than at the saturated liquid state. This can be seen on the T-S diagram of figure 5. As further evidence that this temperature drop occurs we return quickly to psychometrics. Two common parameters it uses are dry and wet bulb temperature. Dry bulb temperature is the actual temperature of the surrounding air. The wet bulb temperature

is the temperature observed after the air has passed through a moist cloth or wick. The wet bulb temperature is always colder. This is because as the air passes through the moist wick it will absorb liquid water as vapor and it must provide the heat of vaporization for this process. Since it provides the heat of vaporization, even though water and air initially presume to be at the same temperature, the air's temperature drops. Proving that heat transfer and temperature alteration can occur by a mass concentration difference alone and with no temperature gradient. In the Joule-Thomson process the liquids temperature drops with no heat transfer and only work input, as explained. Even though the psychometric and Joule-Thomson temperature drops occur by different principles it confirms the ideas regarding concentration difference, evaporation, and temperature. This will all reoccur in the following discussion. The previous process's, with the exception of Joule-Thomson, are called non-equilibrium processes as they do not occur in vapor dome two phase equilibrium.

When our ammonia refrigerant enters the evaporator it is sub cooled at 20°C and 10bar, which is total system pressure. Upon entering the evaporator and combining with the returning hydrogen and ammonia gas, its partial pressure drops. However the ammonia liquid is still subject to the full 10bar of gas pressure above it. But we still say that its pressure is lower as the gases sum by Dalton's law to produce the total pressure above it, and the ammonia gas makes up a low amount of this total pressure initially. Now, at 10bar of pressure the ammonia liquid will not evaporate until 24.89°C , so with a refrigerator compartment of 3°C this evaporation will obviously not occur by conventional means. Despite the fact of the low ammonia partial pressure, the liquid is always under the same pressure.

But as we established discussing mass diffusion, the liquid interface pressure will be that of saturation for the given temperature. So, at 20°C we will have a vapor pressure at the liquid

interface of 8.5762bar. We know that during absorption most of the ammonia is removed from the gas, so the returning gas is largely hydrogen. The exact amounts can only be experimentally determined, but a reasonable guess is 1bar of ammonia pressure and 9bar hydrogen pressure. Thus we will have a concentration gradient of ammonia gas molecules. A diffusion process will begin, or a thermodynamic phase-equilibrium process either way of thinking of it is valid. Heat must be provided for this evaporation process. What subsequently happens is a combination of two effects. The liquid ammonia will draw heat from its surroundings as it simultaneously draws its own heat to provide heat of vaporization. This is not due to pressure loss as in the Joule-Thomson effect, but due to the immediate need for heat as a result of mass concentration difference in the gas. It is easy to confuse the Joule-Thomson expansion with ammonia's mass diffusion when ammonia pressure and temperature drop just as pressure and temperature drops in an expansion. But the mechanism by which these two occur is entirely different. The ammonia is in a multi gas flow situation which is not the same as with a single refrigerant in a valve. We presented the Joule-Thomson effect so as to clearly delineate it from ammonia's mass diffusion; the two processes can be easily mixed up if the details are not entirely known.

So the ammonia now drops in temperature as draws its own, and the compartments, heat and begins to emit vapor. This will continue until the ammonia vapor pressure equals that of the saturation pressure for the current temperature of the liquid. At 20°C we said that the necessary concentration equilibrium pressure was 8.5762bar. But the temperature is dropping and the saturation pressure at the liquid interface along with it. At the same time the vapor pressure rises as the ammonia flows through the evaporator and vaporizes. Using two fictional variables to describe this; temperature, and thus saturation pressure, drops at rate Y while partial pressure increases at rate O. Depending on the exact values of these rates the saturation pressure

necessary and the actual partial pressure of ammonia gas will intersect at some point and the process will come to a halt. The ammonia will now be in temperature-pressure phase equilibrium with its vapor state.

Now, if rate Y is lower than O the process may halt at a higher temperature and thus higher saturation pressure. If say it ended at 3°C, the compartment temperature, the final ammonia pressure in the gas will be 4.8bar approximately up from 1bar initially. If rate O is significantly lower the final temperature will be lower. Say it is -14°C, the final pressure will be 2.5 bar. Which case is better? If rate Y is lower we are evaporating more liquid ammonia during the initial process than in process O. However, all heat drawn comes from mass diffusion rather than ΔT in this case. In the case of lower rate O, we evaporate less initially but we end up at a state that has a very low temperature with a significant amount of ammonia mass left. Here we have a very low temperature, in most systems it is about -15°C to -20°C. No more diffusion occurs due to pressure and concentration differences. But the ΔT between the compartment and the fluid now comes into effect since diffusion, which drove the early temperature drops and vaporizations, has equalized. The fluid absorbs heat due to simple temperature difference and warms slowly. This again drives its saturation partial pressure at liquid interface to increase, which again causes a concentration gradient. So, heat is drawn again to provide vaporization. Because of the large ΔT at this stage, it is reasonable to assume that the heat of vaporization is provided largely by the compartment. With a large ΔT remaining we can transfer heat at a significant rate, which is advantageous for freezer applications.

Which case is more advantageous, or realistic? Say the liquid eventually reaches 3°C in each case with an equilibrium pressure of 4.8bar. Assuming the same mass of hydrogen in the loop in each case, we should have had roughly the same amount of liquid vaporized. The more

preferable answer, and realistic answer is that of a lower rate O, which was our second case. It is unrealistic that the liquid ammonia could draw in heat so fast as to reach 4.8bar at 3°C or higher without its temperature lowering very quickly. As in the psychometric example of air passing through a moist wick, the air provides the immediate heat for the vaporization and drops in temperature. This is in spite of the fact that it can draw heat from the surroundings. The additional advantage of case O, is that we end up at a lower temperature. Because of the large ΔT , we can pull in heat at a higher rate as the ammonia partial pressure gradually increases. This is needed if we have a freezer cabinet that we need to maintain at around 4°F. In reality the rates, Y and O, are not something that can be altered as we please. The ammonia liquid will evaporate at the rate determined by the laws of concentration diffusion and thermodynamic phase equilibrium. Y and O serve to explain how we arrive at the states explained. To further demonstrate this we refer to figure 12 and figure 13 below:

when saturation pressure of temperature and partial pressure equalize. Beginning again at state 4c, the cold ammonia now begins draw heat by conventional transfer methods and warms and releases more ammonia vapor increasing to a final partial pressure of 3.6bar in their system. The numbers will vary system to system but the effects are all the same. To demonstrate that the 2.1bar value reached is not simply the initial partial pressure of the returning hydrogen/ammonia mixture, and that the actual cooling does not occur by Dalton's law, we present a second T-s diagram.

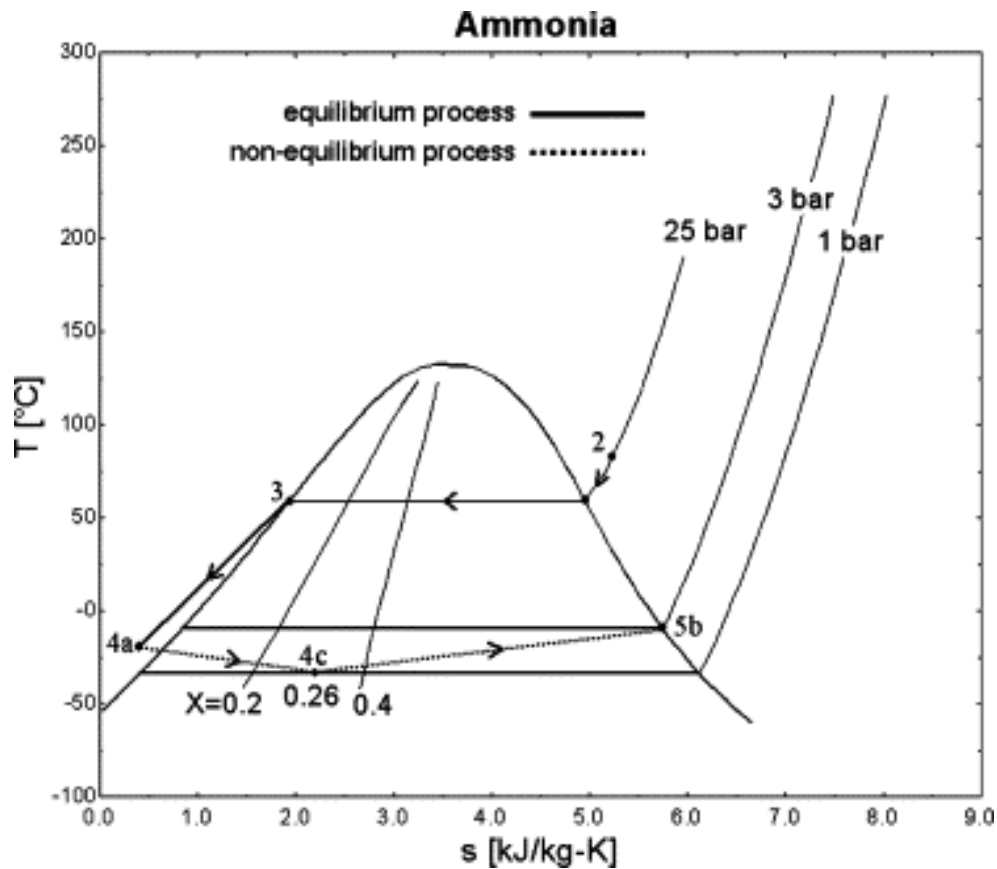


Figure 13 T vs. s diagram of ammonia cycle with pre-cooling

This one models the same system, but with pre-cooling of the condensate liquid added. This pre-cooling occurs from 3-4a. This is done for two reasons, one is that the liquid is warm when it enters; 20°C in our case and 52°C in theirs. So the liquid can initially transfer some heat

out to the compartment, we want to prevent that. The second reason is that by pre-cooling the liquid ammonia enters at a very cold temperature as seen, and as a result its saturation pressure at liquid interface is much lower. This means it needs to evaporate far less ammonia initially and cool less to reach partial pressure-saturation pressure equilibrium. We can see in the pre-cooling diagram that it reaches equilibrium at 1 bar of partial pressure at state 4c. For this to be so, would confirm that the partial pressure of the ammonia when it returns from the absorber loop must be very small. This demonstrates again that vaporization does indeed occur while cooling is occurring. It is interesting to note that the study done which generated these diagrams found that the non-pre-cooled system operated more efficiently. The pre-cooling cycle required excess heat to be transferred to cooling the condensate and left little for cooling the compartment. Below is a diagram of the non-pre-cooled system for reference.

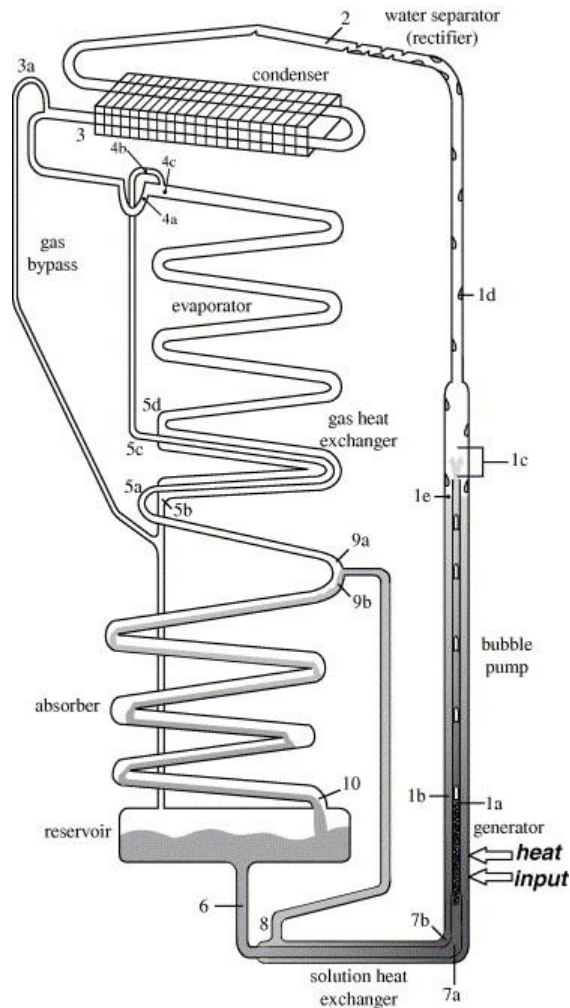


Figure 14 System diagram for accompanying T vs. s chart without pre-cooling

So, in lieu of the above explanations what does this mean for our formal mathematical analysis? To model the process accurately would require a combination of mass diffusion, thermodynamics, heat transfer, and general fluid flow considerations. We can describe the states that it goes through, but when you have a mass diffusion scenario that is not at constant temperature, and not at constant concentration difference, you end up with differential modeling scenario. Coupling that with the unknown rates Y and O , and changing mass and flow speed of liquid and gas through the evaporator coil as one decreases in mass and the other increases respectively, gives us a very complicated situation to model. We can simplify certain aspects of

it; we could assume equal temperature and only model concentration gradient. Or perhaps we could model it as a liquid in a fixed position vessel with an unchanging gas composition moving over it. In either case we will have a very simplified model from the real situation. To make a highly accurate model would go beyond the scope of this project and into other disciplines. To determine the proper sizing we decided to use a standard analysis. We modeled it as single refrigerant in a conventional refrigerator which is a two-phase equilibrium evaporation situation. We used:

$$Q = \dot{m} * \Delta h_{sp}$$

$$L = \frac{Q}{\pi * D * h * (T_R - T_p)} = \frac{\dot{m} * \Delta h_{sp}}{\pi * D * h * (T_R - T_p)}$$

to model the total heat flow and mass flow rate. This was presented in our refrigerator compartment section. We chose a pressure of 3.552bar with a temperature of -5°C for the ammonia refrigerant. We selected this as we believed that 8°C would be a satisfactory ΔT to provide an adequate cooling rate and short pipe length. With a heat flow into the box of 1.64watts as found earlier, and a Δh_{sp} of 1279.56KJ/kg at 3.552 bar, we solve for a mass flow rate of:

$$\dot{m} = 1.27 \times 10^{-6} \frac{kg}{s}$$

This is a very small rate, but is mathematically accurate. In reality we could not achieve such an exact figure of flow rate, but theoretically it is valid. This flow rate of ammonia will be fixed throughout the system and will be utilized in our subsequent generator analysis. Next, analyzing the length, we again approximated fluid temperature to be that of the pipe temperature

as the tubing we are using is only 0.028in thickness. With a low guess of 5, for internal convection coefficient between the pipe and surroundings we solved for L with the equation below:

$$L = \frac{Q}{\pi * D * h * (T_R - T_p)} + 0.2 * \frac{Q}{\pi * D * h * (T_R - T_p)}$$

This is a modified form of the equation presented in the cabinet section. We have added the second term to represent an additional 20% length. We added this to have a 20% margin of error in our length determination. There are always inefficiencies and data errors in any analysis, the error margin we factored in should cover this. With the following values we computed length to be:

$$h = 5 \frac{W}{m^2}$$

$$Q=1.64 \text{ watts}$$

$$D=.00952m$$

$$T_R=296.15K$$

$$T_P=268.15K$$

$$L=1.64m$$

This is the length that we settled on and built into our evaporator section of the completed system.

ABSORBER

The main purpose of the absorber is to separate the refrigerant from the third fluid, which in our case is the ammonia from the hydrogen gas. In order for steady state to be achieved, all of the ammonia coming from the evaporator must be absorbed by the water through diffusion. The ammonia comes out of the evaporator at a specific mass flow rate which can be found using the equation below.

$$Q = \dot{m} * \Delta h_s$$

The heat transfer variable of this equation is equal to the heat transferred from the surrounding to the cabinet, which we found in the *Refrigerator Cabinet* section. The change in enthalpy is equal to the heat of vaporization of the ammonia refrigerant at -5°C. We obtain a mass flow rate of

$$\dot{m} = 1.28\text{E-}6 \text{ kg/s}$$

So we need an area big enough to facilitate absorption of ammonia at a rate of 1.28E-6kg/s. Our absorber is made out of a cylindrical pipe 6 inches in diameter and 1 ft in length with caps at each end, giving plenty of cross sectional area for the absorption of ammonia in water.

The liquid water returning from the separator will be at higher elevation and flow downward to the absorber. The warm gases entering the absorber will enter the side piping of the absorber and begin to flow upward due to buoyancy force. The liquid water and warm ammonia gas will thus counter flow and in the process combine to form our solution. The combined liquids then flow downward back to the absorber. The best way to ensure this is to connect the water return pipe to the top side of the absorber side pipe. This will bring water down across the flowing gases.

We need the water to be at 20°C to combine in the proper fractions. So we must compute the proper length required for this to occur. The liquid will be a mixture of vapor and liquid that

reached 110°C as well as being elevated before reaching generator temperature. Analyzing enthalpy change between these points, we have, $\Delta h = 377.34 \text{ KJ/kg}$. Multiplying by 1000, to convert to joules, and times mass flow rate we find a heat transfer of 0.479 watts. This heat transfer produces an insignificant distance given the high midpoint ΔT , making this section of pipe a lesser design concern.

The gases must also be prevented from entering the separator so that it does not contaminate the pure ammonia side of the system. To prevent this we use a U-bend near the entrance of the separator. This establishes equilibrium liquid level across the bend, and prevents any gas from traveling back up the tube. After proper combination of the fluids at the appropriate temperatures, the liquid solution flows back down to the absorber and into the generator.

Condenser Analysis

Presuming the proper gas flow rates are established and the separator functions properly, we will have pure ammonia gas at a mean temperature about 110°C entering the condenser. We must calculate the proper length. This length is that which is necessary to condense the fluid back to room temperature in the liquid state.

To analyze we must evaluate length of three region of heat transfer. The initial region where the gas condenses from superheated gas to the saturated vapor state, the second region where it goes from saturated gas to saturated liquid, and a third region where it goes from saturated liquid to sub cooled liquid. We can't analyze these as one region with a ΔT of 90°C because the enthalpy change with temperature is not linear. It is substantially higher in the two-

phased vapor-dome. So we analyze in individual sections. To model the lengths, we reuse our equation for length from the first section.

$$L = \frac{(Q)}{\pi * D * h * (T_R - T_p)} = \frac{(\dot{m}) * (\Delta h_{sp})}{\pi * D * h * (T_R - T_p)}$$

We know all of the necessary values except Q, or $\dot{m} * \Delta h_{sp}$. In a pipe with a progressive temperature change as it cools we have a changing heat transfer rate. To find the rate that represents the overall surface area necessary, we would normally need to use a differential equation. But, as a reasonable approximation we use the midpoint temperature of the fluid of the temperature change ΔT . We evaluate L using this point.

In our superheated region we go from 110°C to 24.89°C, which is the saturation temperature of ammonia at 10 bar. The midpoint temperature is 67.445°C. Making the approximation the fluid temperature equals the inner wall temperature and the inner wall temp equals the outer wall temp, since our wall thickness is only 0.024 inches, we know our value of $(T_R - T_p)$. Total Q, is determined by mass flow rate times change in enthalpy. Mass flow was previously found, and change in enthalpy from thermodynamic tables is 121.22 KJ/kg. Using:

$$h_2 = 8 \text{ W/m}^2\text{K}$$

we get a length of:

$$L_{1c} = .025805\text{m} = 1.015 \text{ inches}$$

Because of our extremely low mass flow rate the fluid condenses quickly to saturated gas. The distance is so small will need to add insulation to the pipe exiting the separator to ensure the ammonia does not condense and flow back to the generator.

Performing similar analysis in the saturated region we resolve. Temperature is roughly constant in this region, at about 24.89°C. So we know our ΔT between pipe and ambient air. Using thermodynamic tables we get a Δh_{sp} of 1165.42 KJ/kg. Calculating length we get:

$$L_{2c} = 1.272 \text{ m}$$

The third region, the sub cooled region has very small change in enthalpy. We evaluate enthalpy at the saturated temperature of the liquid as part of the incompressible substance model. Over the 4°C from 24.89°C to 20°C our Δh_{sp} is only 23.56 KJ/kg. This produces insignificant heat transfer and a length that may be neglected. So our ideal total condenser length is:

$$L_c = 1.2978 \text{ m}$$

But when we factor in an error percentage of 20% for the actual surface temperatures of the pipes we get:

$$L_c = 1.557 \text{ m}$$

Now, to provide a further error margin we recomputed the above numbers for the lowest possible convection coefficient of air 5 W/m²K. Doing so and recalculating the error percentage we get a condenser length of :

$$L_c = 2.458 \text{ m}$$

In any refrigeration system we should be rejecting more heat than the refrigerator takes in. Even in an ideal system. Heat input to the refrigerator was found to be 1.6345 Watts. Taking mass flow rate of the three regions of the condenser above and multiplying by the respective changes in enthalpy we get a heat rejection from the condenser of:

$$Q_{out} = 2.0954 \text{ watts}$$

So we are releasing more heat from our system than we are inputting as expected.

Also, to prevent the hydrogen from flowing into the condenser, we place a U-bend in the circuit. The U-bend will maintain an equal liquid level across it. As liquid builds on one side, it will force the liquid level up on the other side, so equilibrium is always maintained. This means

that we have a liquid barrier through which the hydrogen at 6.4 bar cannot pass. We must contain the hydrogen to proper side of the system.

Generator Analysis

The generator provides the power to drive the system. Its' general functioning is as follows: ammonia-water solution enters the generator from the absorber at a certain mass fraction. Then heat is applied to vaporize the ammonia and leaves a weak ammonia solution behind. The rising vapor elevates the solution through the bubble pump to the separator, where the weak ammonia solution can drain out of the other side of the separator to the absorber. The ammonia vapor then exits through the top of the separator and proceeds on to the condenser.

We begin with a basic explanation of the concentration fractions involved in the generator. When liquid solution enters the generator, the liquid flow will follow different paths. As in any fluidic system the flow will have path lines that it follows. As it enters the generator some of the flow will be pulled in close contact with the heated point, and some will be pulled above and receive minimal heating. The flow, which is heated sufficiently, releases ammonia with a weak water concentration in gas form. This gaseous mixture elevates the liquid through the bubble pump. The ammonia vapor then escapes through the separator. The liquid, which has been elevated, is a mixture of flows, some of which were fully heated, partially heated, and almost non-heated. Each of these flows will differ in fractions of ammonia. This is because it takes very little vapor to elevate liquid in a tube or column. So not nearly all of the ammonia needs to be vaporized to induce liquid flow up to the separator through the bubble pump. To drive more ammonia out we reheat the solution in the separator. This reduces the fraction of ammonia returning to the absorber through the liquid return pipe significantly. All commercial systems have a method of reheat, typically with an electric coil. The book Absorption Chillers

and Heat Pumps by Herold, Radermacher, and Klein, states that in typical commercial gas absorption units the liquid returning to the absorber from the separator typically contains a 0.1-0.2 mass fraction of ammonia. This is due to inefficiency of uneven heating.

To show the initial fraction entering we refer to the chart below.

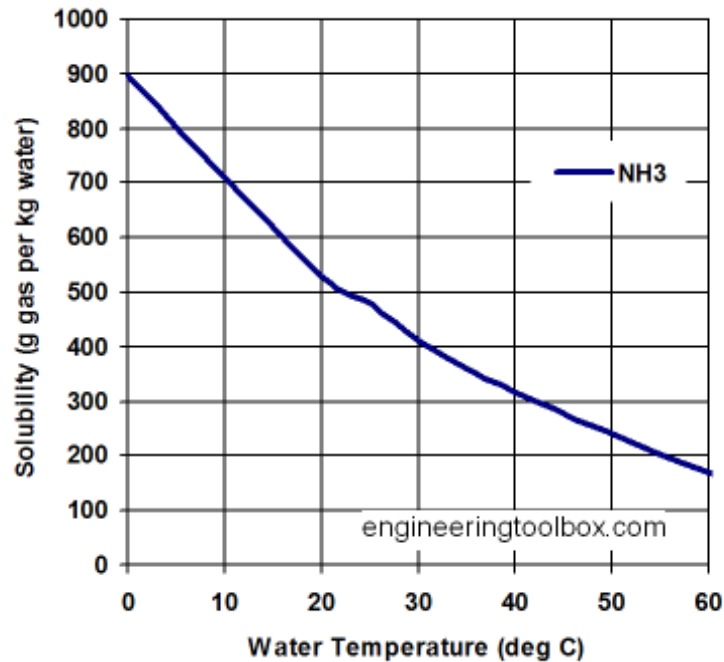


Figure 15 Solubility graph of ammonia in water

According to the chart at 20°C, the temperature at which our absorption should take place, we should have 520 grams of ammonia in 1000 grams of water. Using the simple formula below we get an ammonia fraction of solution by mass:

$$X = \frac{m_a}{m_w + m_a}$$

Computing the fraction we get: 0.342 kg of ammonia/kg solution.

Now we know that we need a mass flow rate of 1.28E-6 kg/s of ammonia through the system consistently. That mass flow of ammonia must be entering along with a certain mass flow of water. In the ideal case with all ammonia driven out and escaping we can compute the

necessary water flow rate by simply rearranging the above equation to solve. It works the same with fixed mass as with flowing mass.

$$\dot{m}_w = \frac{\dot{m}_a}{X} - \dot{m}_a$$

But, we know that there is inefficiency so a given fraction of ammonia will not escape. It will circulate back around again. The high value given in Absorption Chillers and Heat pumps was 0.2. Assuming our system to be of low efficiency compared to commercial units, we will take the high value of unused ammonia for our system, 0.2. Now, since a fraction of ammonia is not recirculating we need a greater flow rate of ammonia than $1.28\text{E-}6$ kg/s total at steady state operation to supply the system. To find the proper flow rates we utilize forms of the above equations.

At steady state we have approximated an exit fraction of 0.2. So, using the mass fraction equation from before, we set it equal to 0.2 and solve for the fixed mass of ammonia, labeled m_{af} , that will be constant in the generator/absorber loop. To do so we analyze in terms of mass present and find mass flow later. The masses used are 1000grams of water and m_{af} grams of fixed ammonia mass. This will give us ratios which we can use later to find flow rates. Solving for m_{af} at return pipe entrance we get:

$$m_{af} = \frac{X_e * m_w}{(1 - X_e)}$$

Using:

$$X_e=0.2, m_w=1000$$

$$m_{af}=250$$

Now, returning to the entrance to the generator before any ammonia has been heated we have a normal fraction of 0.342. This required 520 grams of ammonia per kg of water. By simple

subtraction this means that we need 270 grams of escaping, or non-fixed, ammonia mass per cycle. We know that the system ammonia flow rate that we need is 1.28E-6kg/s. So using this as our known variable we can solve for the proper mass flow rates of the water and fixed ammonia. The full fraction equation is:

$$X = \frac{m}{m_w + m_{af} + m_a}$$

We first obtain the overall fractions of the mass with our know values. Substituting in m_w , m_{af} , and m_a form in the numerator in the above equation we get the fraction of the total flow that each component constitutes. The results are:

$$X_a=0.17763$$

$$X_{af}=0.1644$$

$$X_w=0.6579$$

Now, again using the full fraction equation we can find mass flow rates since we have a known \dot{m}_a . The procedure is to substitute the known fraction of the water or fixed ammonia flow that we want to find for X, and then the variable in the numerator and rearrange to solve. Since we have two unknowns we get the following equations:

$$\dot{m}_w = \frac{X_w * (\dot{m}_{af} + \dot{m}_a)}{(1 - X_w)}$$

$$\dot{m}_{af} = \frac{X_{af} * (\dot{m}_w + \dot{m}_a)}{(1 - X_{af})}$$

By substitution of \dot{m}_{af} into the \dot{m}_w equation and doing out the algebra we got an equation for the mass flow rate of water:

$$\dot{m}_w = \frac{X_w * \dot{m}_a}{(1 - X_{af}) * (1 - X_w) - (X_w) * (X_{af})}$$

With this we can then solve for mass flow of fixed ammonia. Using the known fractions, along with our mass flow rate we got:

$$\dot{m}_a = 1.28\text{E-}6 \text{ kg/s}$$

$$\dot{m}_{af} = 1.18\text{E-}6 \text{ kg/s}$$

$$\dot{m}_w = 4.76\text{E-}6 \text{ kg/s}$$

$$\dot{m}_{total} = 7.18 \text{ E-}6 \text{ kg/s}$$

Substituting these into the full X equation will produce the correct mass fractions. These will be used later when we evaluate the generator in detail.

Now, to properly evaluate the heating process of ammonia we must explain certain details of it first. Figure 16 below is a diagram of Temperature vs. mass fraction for a general zeotropic mixture. A zeotropic solution is defined as one for which the mass fractions in phase equilibrium for vapor and liquid are always different. Most solutions are zeotropic. Figure 16 shows two lines, the boiling line and superheated line, which the diagram calls the dew line. The boiling line is later referred to as the auxiliary line. Below the boiling line is the sub cooled region. Here the solution is in liquid form. The heating process is as follows. The fluid at initial liquid temperature T_1 , indicated by state 1' on the diagram is heated until reaching the boiling line at state 2'. With a traditional pure substance the fluid would then proceed through a two phase region at constant temperature with varying quality until reaching pure vapor. A zeotropic mixture does not work this way. As vapor releases mass fractions change and temperatures must therefore change.

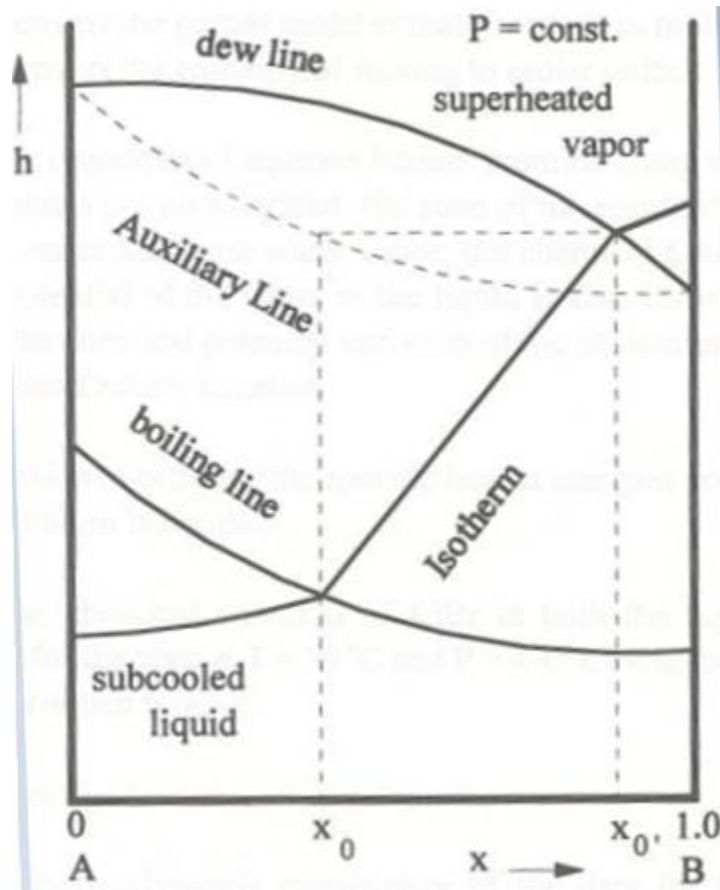


Figure 17 Enthalpy vs. concentration diagram

The above diagram is an enthalpy vs. concentration diagram, similar to the temperature vs. mass fraction diagram of before. It is representative of an alternate process to evaluating zeotropic solution heating. We again see a dew line and boiling line, but this time we have an additional line. The auxiliary line is used to find the mass fraction of escaping vapor along with its enthalpy. We again utilize isothermal lines to find X of the vapor at the current boiling state. But, to be able to find the isothermal lines we must use to isostere's intersection with the auxiliary line. An isostere is a vertical line of constant mass fraction.

First, we make clear what all the lines are. The boiling line is the same as previous; it is the border between sub cooled solution and the initial point of vapor boiling. The dew line is again the line of pure vapor, the intersection of the isostere with the dew line tells us the total

enthalpy if all solution is vaporized. The auxiliary line however, is a line of the properties of the initial vapor released at a heating point. These were given as states 2'', 3'', and 4'' previously. Then we just used it to find the escaping fraction, but it is also used on the h-x diagram to give us the enthalpy of the escaping vapor. So, the auxiliary line and the boiling line actually coincide. When boiling is reached the simultaneous enthalpy of liquid and escaping vapor are read off the h-x diagram by the isostere. But to find X of vapor we must again use isothermal lines. These isothermal lines are found by following a line of constant enthalpy to the right from the intersection point of the current mass fraction and the auxiliary line. The fraction of vapor is then the isostere to this point. This is shown on the diagram. As a final note, if we look at the two vertical axes, we see that the isothermal lines at these points would become vertical, indicating the proper heating relationship for pure substances.

To analyze our system we utilized an h-x diagram. We utilized the above processes to obtain the proper enthalpies at entrance and exit. The diagram with the proper lines is on the following page. Our system has an initial fraction of 0.342. We then made the presumption of a low efficiency heating and an exit fraction of 0.2. This gives us our two isostere's to read from. By reading only the 10 bar pressure lines the chart becomes identical to the example one above. Using the auxiliary line we traced the proper isothermal lines to find mass fraction of vapor at the initial and final points. We then read off enthalpy of sub-cooled liquid, saturated liquid, saturated vapor, and temperature at the two isostere's. Our resulting values were:

$$X=0.342$$

$$X_e=0.2$$

$$h_{\text{sub(sp)}} = -125 \text{ KJ/kg} = h_{\text{sp1}}$$

$$h_{\text{L(sp) saturated}} = 200 \text{ KJ/kg}$$

$$h_{L(sp) \text{ saturated}} = 398 \text{ KJ/kg} = h_{2sp}$$

$$h_{v(sp) \text{ saturated}} = 1525 \text{ KJ/kg}$$

$$h_{v \text{ saturated}(sp)} = 1785 \text{ KJ/kg}$$

$$X_v = 0.95$$

$$X_v = 0.800$$

$$T = 93^\circ\text{C}$$

$$T = 128^\circ\text{C}$$

The original chart we used, which contained all the lines of interest on it in the form of a T-x diagram, has the boiling and auxiliary lines coinciding along an isobar as they really do. It does not show the dew line enthalpy. This chart will confirm all of the properties above. It is located in appendix 1.

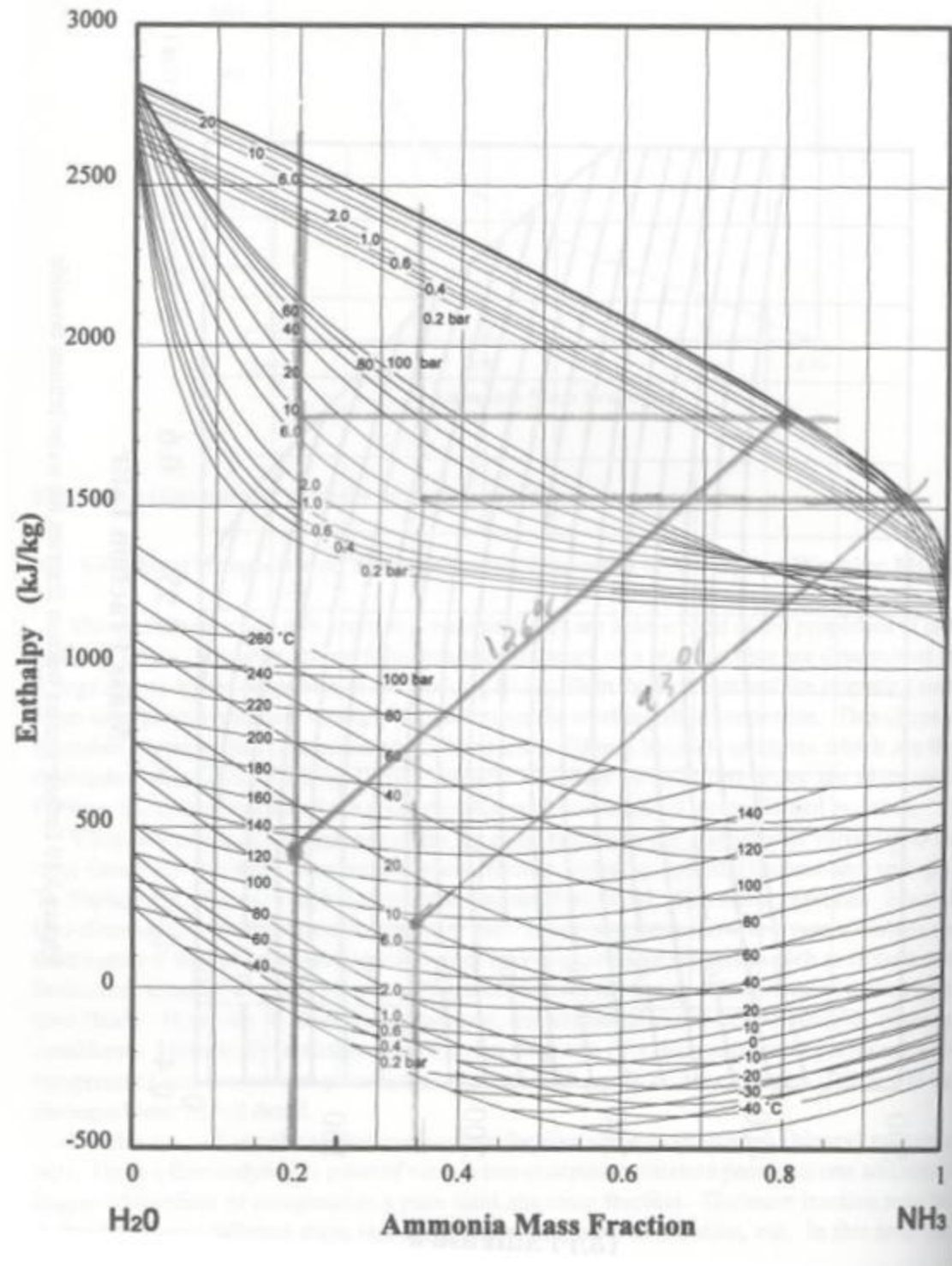


Figure 18 Enthalpy vs. mass fraction of ammonia

Now, we analyze the generator entire cycle's theoretical performance. We now know our mass flow rates and enthalpies which gives us everything we need to analyze performance. We have two exits and one inlet; by using the first law of thermodynamics we obtain a general heat input equation:

$$Q - W = \dot{m}_3 * \left(h_{3sp} + \frac{v_3^2}{2} + g * Z_3 \right) + \dot{m}_2 * \left(h_{2sp} + \frac{v_2^2}{2} + g * Z_2 \right) - \dot{m}_1 * \left(h_{1sp} + \frac{v_1^2}{2} + g * Z_1 \right)$$

Neglecting velocity and potential gravity, along with work, we get:

$$Q = \dot{m}_3 * h_{3sp} + \dot{m}_2 * h_{2sp} - \dot{m}_1 * h_{1sp}$$

State 3 we take as our vapor which escapes into the separator, State 2 we take as the returning liquid solution, and state 1 is the entering solution. For the enthalpy h_{3sp} we must take the median of our two vapor enthalpies. This is because vapor is released at constantly varying fraction along the line between then. So the enthalpy will vary from 1525 to 1785, taking the average we get $h_{3sp}=1655\text{KJ/kg}$. Now, for mass flow at state 3 we will use an altered \dot{m}_a from before. This will include the water vapor in the 0.87 average ammonia concentration exiting. The vapor water flow is:

$$0.87 = \frac{\dot{m}_a}{\dot{m}_a + \dot{m}_{wesc}}$$

Solving for escaping water we get:

$$\dot{m}_{wesc} = 1.91\text{E-}7 \text{ kg/s}$$

Then subtracting this flow rate from the water flow at state 2 we then have:

$$\dot{m}_w(\text{modified}) = \dot{m}_w - \dot{m}_{wesc} = 4.54\text{E-}6 \text{ kg/s}$$

So, \dot{m}_a and \dot{m}_{af} have not changed.

Using these new values our three mass flows are:

$$\dot{m}_3 = 1.47\text{E-}6 \text{ kg/s}$$

$$\dot{m}_2 = 5.72\text{E-}6 \text{ kg/s}$$

$$\dot{m}_1 = 7.18\text{E-}6 \text{ kg/s}$$

With h_{sp2} and h_{sp1} previously given we now compute:

$$Q = (.000001468)(1655)(1000\text{J/KJ}) + (.000005715)(398)(1000\text{J/KJ}) - (.000007184)(-125)(1000\text{J/KJ})$$

$$Q = 5.602 \text{ Watts}$$

With Coefficient of performance defined as the ratio of watts of cooling to watts of power input we get a theoretical COP of:

$$COP = \frac{Q_{in(e)}}{Q_{in(g)}}$$

$$COP = 1.6345/5.602$$

$$COP = 0.292$$

This falls in line with most gas absorption refrigeration cycles.

Finally, the limited water vapor that does escape will quickly condense and flow back down to the liquid. This is because the vapor is on average only 0.13 by mass of the exiting vapor flow. So, it therefore constitutes only about 1.5 bar of partial pressure of the escaping gases. At this pressure it has a saturation temperature of 111.4°C. With an ambient temperature of 20°C, the difference in temperature will be large enough to cause the water vapor to re-condense fairly quickly. This raises another issue with the escaping ammonia vapor. It will be around 9 bar of pressure initially and 10 bar after the water condenses. It will then condense at 24.89°C. In the next section we compute the length that the ammonia will begin to condense at, but to state the result now, it is very small. This same situation occurs in the bubble pump tube. The gaseous ammonia will be surrounded by partially heated liquid water, and an ambient

temperature of 20°C. There is the possibility that heat could conduct out very quickly and cause the ammonia to recondense. With no vapor flow, the bubble pump would shut down. In Absorption Chillers and Heat Pumps, they describe this effect occurring in a test unit when heat input dropped below a certain level. The two solutions were to increase heat input, and to add insulation to the pump tube. Given the low power of ours, adding insulation may become a necessity. This will be determined during testing.

System Theoretical Performance

The generator section above explained in detail the process of analyzing the thermodynamic properties of a zeotropic mixture. We then explained the method of obtaining mass flow rates and enthalpies, and then finally the heat input and coefficient of performance. We now analyze the optimization of the generator and overall system. To do this we vary mass fractions at entrance and exit, and therefore heating temperatures and mass flow rates, to examine the effect on COP that this has. To do this we took the equations and analysis methods of the previous section and created a Mathcad file. We created formulas for all seven necessary flow rates. These being the three solution flow rates of water flow, fixed (or recirculating ammonia), and ammonia flow. The other four are made up of the three flow rates into and exiting the generator, labeled one two and three and used in the equation for Q , and the mass flow of the limited amount of water vapor that escapes. If one follows the generator analysis step by step, you can see that the first condition we need to specify to be able to subsequently analyze all others is the exiting mass fraction at point 2. Once this is specified, we can find the ratios of the three components to each other at the entrance, which is point 1. Then with our mass flow of ammonia being considered a constant, which is determined elsewhere in the system, we can solve for the mass flow rates of the other two components. Once these are

known we need to then look up the proper enthalpies at these fractions of solution. In order to be able to view a graph of the results as exiting fraction varied, we had to take data points of liquid and vapor enthalpies vs. mass fraction of solution. We then used Excel to graph and curve fit the data with a polynomial function to the 5th power. With these known, we then simply added functions to obtain mass flow at points one two and three. Obtaining graphs of Q, and COP was then simple. So, essentially all our graphs and results were a function of exiting mass fraction X_e . With \dot{m}_a and the mass fraction at the entrance being constant, X_e is our variable.

Theoretical Results:

We specified our variable X_e , to range from zero to 0.342, which is our entrance fraction. So results for COP and Q vary with no ammonia escaping when X_e is close to 0.342, to all of it escaping at $X_e=0$. Resulting graphs with entrance fraction $X=0.342$ are below:

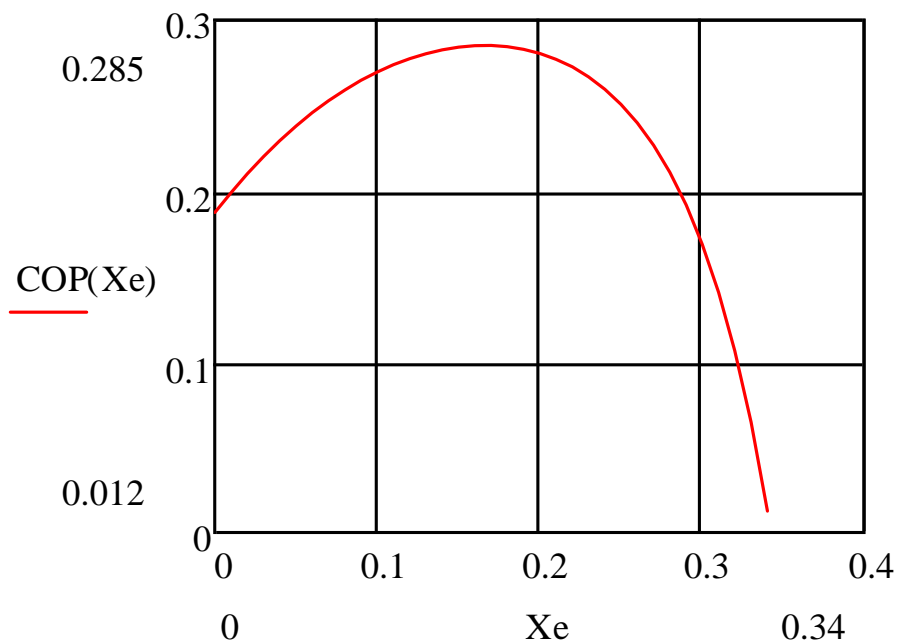


Figure 19 COP vs. mass fraction

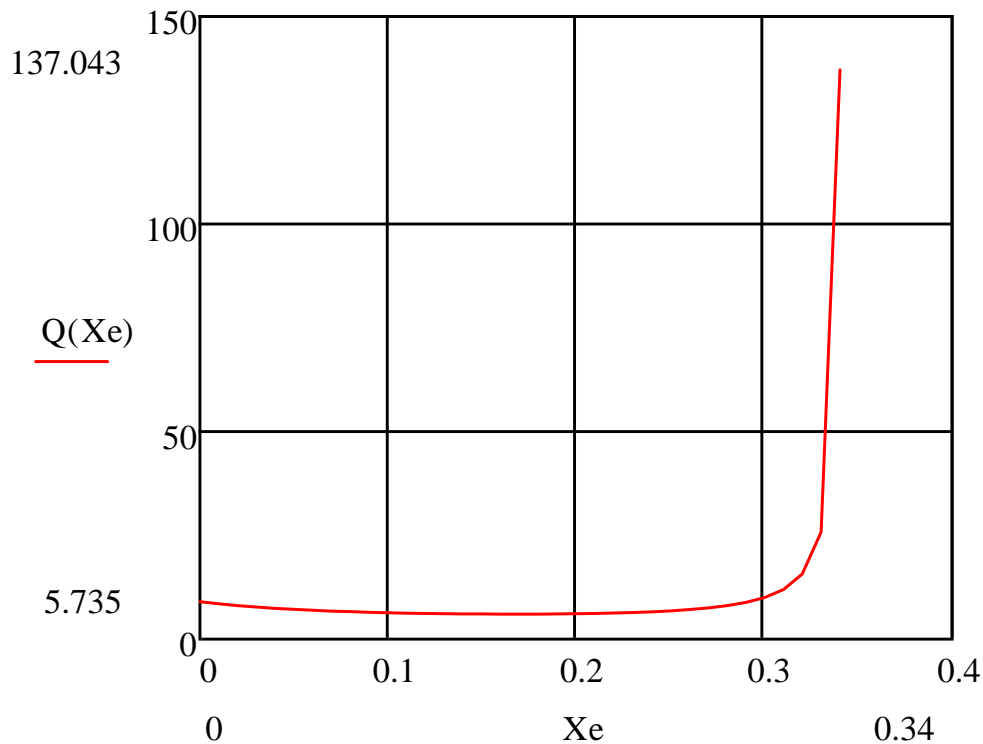


Figure 20 Q vs. mass fraction diagram

The results shown above indicate that our previous generator section analysis was fairly accurate. Previously we calculated COP at $X_e=0.2$ and obtained 0.292, here we see a value of about 0.280. The error margin is caused by the curve fitting function we used for the enthalpies, whereas previously we simply read off the graph the particular point we were interested in. That being said, the results indicate several interesting things. We see that we have an optimum point of operation, where heat and COP are minimized and maximized respectively. One's first thought might be that the optimum idea would be to heat away all the ammonia and therefore have to recirculate less of it. But this is not true. The closer the exit fraction approaches to zero the more heat input is necessary. If one examines the Enthalpy vs. Fraction diagram we used in the previous section you can see the enthalpy of vapor, and to a lesser extent liquid, curves up sharply as exit fraction approaches zero. Thus the heat input necessary increases significantly,

but goes to a finite point. At the high exit mass fractions we also see low efficiency. This is because at low ammonia loss we require much higher flow rates to maintain the $1.28\text{E-}6\text{kg/s}$ of ammonia flow escaping that we need. These flow rates, although technically finite, approach infinity as X_e approaches X . Shown below is a graph of mass flow at the entrance point.

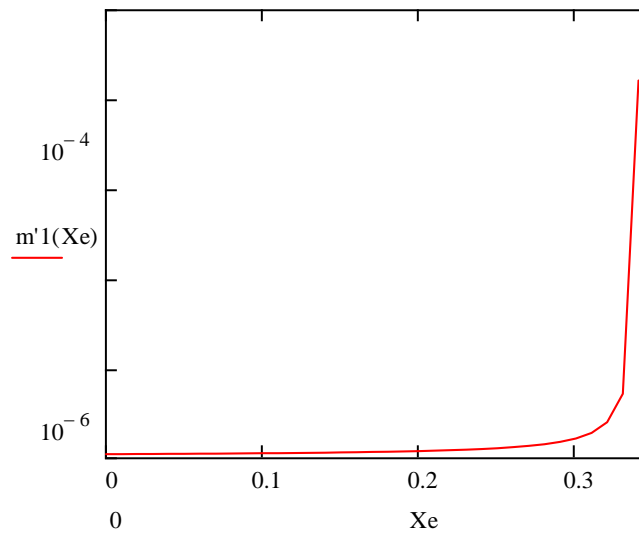


Figure 21 Mass flow diagram

The mass flow at exit, point 2, also follows this type of curve. So, clearly at the higher exiting mass fractions it is mass flow that causes our higher necessary heating values. The simplest way for one to understand this is if you think of water flowing very fast through a pipe. Say it is heated over only a foot of length. Then, to evaporate it when it is flowing fast you would naturally need a very high rate of heat input compared to a slow moving flow.

$$Q = \dot{m}_3 * h_{3sp} + \dot{m}_2 * h_{2sp} - \dot{m}_1 * h_{1sp}$$

Seeing the equation assists in understanding the COP and Q graphs. From $X_e=0.342$ to the optimum point mass flow rates \dot{m}_2 and \dot{m}_1 drop at a greater rate than the contribution to heat due to enthalpy rises (Note, h_{1sp} is a negative value so \dot{m}_1 and h_{1sp} form a positive number). The situation is reversed after the optimum.

As a final note, the optimum compromise between mass flow and enthalpy is actually a benefit to some degree. This means that if we have a waste heat source for example, we will not need it to be as high a temperature as possible. It will only need to heat to about 130°C in the case of the model used above. How might we increase efficiency such that the necessary temperature is even lower and COP increases even further. Professional absorption systems run in the range of 0.6 to 0.8 efficiency, so our maximum of 0.285 above is too low.

Improving System Efficiency

The first and simplest way to increase performance is to perform heat exchange. This heat exchange is used in nearly every two and three fluid absorption system. What this does is exchange heat between the cool entering solution and the hot exiting solution. So, effectively the heat at point 2, Q_2 , is recycled. To model this we used the following equation.

$$Q_{exch} = \dot{m}_2 * (h_{2sp_{1e}} - h_{2sp_{2e}})$$

This is the total heat that the exiting flow can transfer if it goes from its initial exiting enthalpy, $h_{2sp_{1e}}$, down to its enthalpy at room temp, $h_{2sp_{2e}}$. This is an ideal transfer case which typically only occurs in infinite length cross flow heat exchangers. However, this is an ideal analysis so this simplified model is sufficient. We then subtracted Q_{exch} from Q to get net heat input.

$$Q_{net} = Q - Q_{exch}$$

The heat exchanged efficiency was then labeled as COP_2 , and plotted. The results are below.

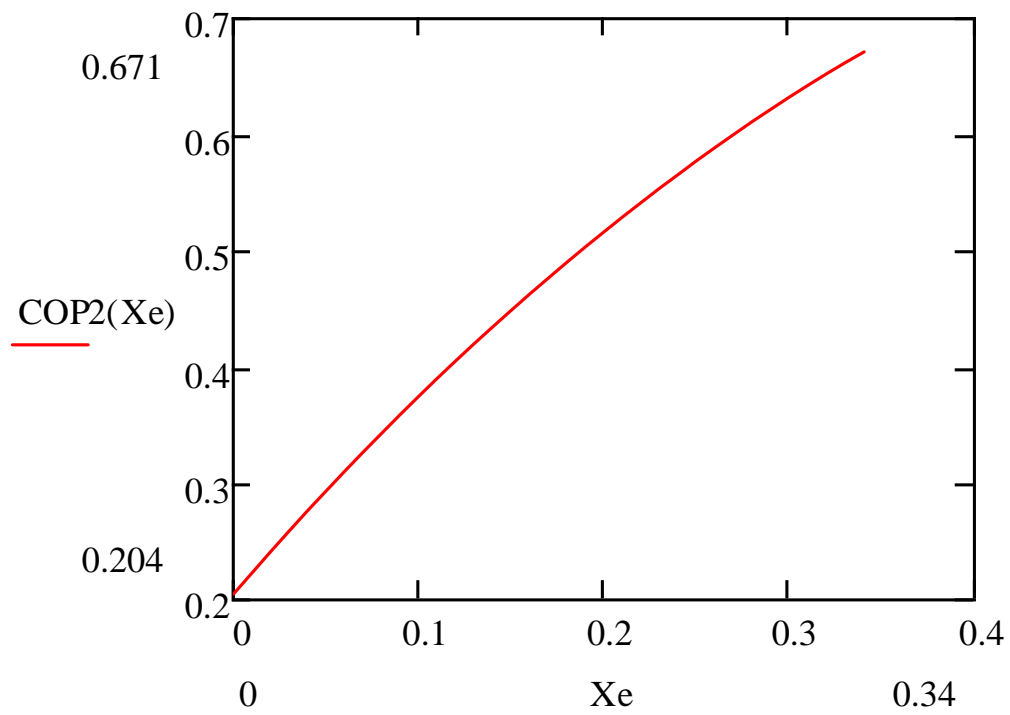


Figure 22 COP with heat exchange. The Max and Min values are listed on the y-axis.

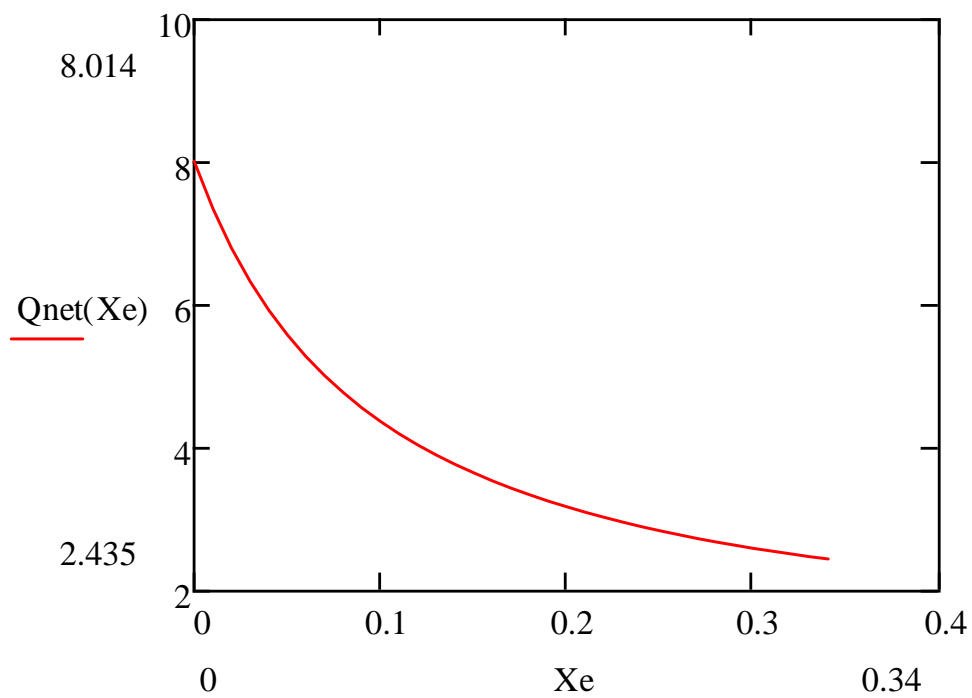


Figure 23 Net heat input Q_{net} . Max and Min are labeled.

These results are initially perplexing. Previously we explained the tradeoff between mass flow and enthalpy that leads to an optimum point but here we have no optimum. The max efficiency occurs when X_e is nearly equal to X , and flow rates are very high. We explain by showing the detailed Q_{net} equation:

$$Q_{net} = Q - Q_{exch}$$

$$Q_{net} = (\dot{m}_3 * h_{3sp} + \dot{m}_2 * h_{2sp} - \dot{m}_2 * h_{1sp}) - \dot{m}_2 * (h_{2sp_{1e}} - h_{2sp_{2e}})$$

$$Q_{net} = \dot{m}_3 * h_{3sp} + \dot{m}_2 * h_{2sp_{2e}} - \dot{m}_1 * h_{1sp}$$

Where, $h_{2sp_{2e}}$ is state 2 after heat exchange.

Beyond approximately $X_e=0.1$, both h_{2sp} and h_{1sp} are negative, and on the order of 0-100KJ/kg. As X approaches X , at 0.342, $h_{2sp_{2e}}$ approaches h_{1sp} . So the enthalpies are virtually identical. Previously we showed a curve of \dot{m}_1 vs. X_e , and then stated that \dot{m}_2 followed a similar curve. It does, and consequently their values are on the same order of magnitude with each other. The values are of course different, but nevertheless similar. Thus with \dot{m}_1 and \dot{m}_2 very close, and $h_{2sp_{2e}}$ and h_1 very close, the two heats tend to cancel each other out. This leaves $\dot{m}_3 * h_{3sp}$ as the dominating factor in Q_{net} . Below is the resultant graph of Q_3 , which is the product of \dot{m}_3 and h_{3sp} .

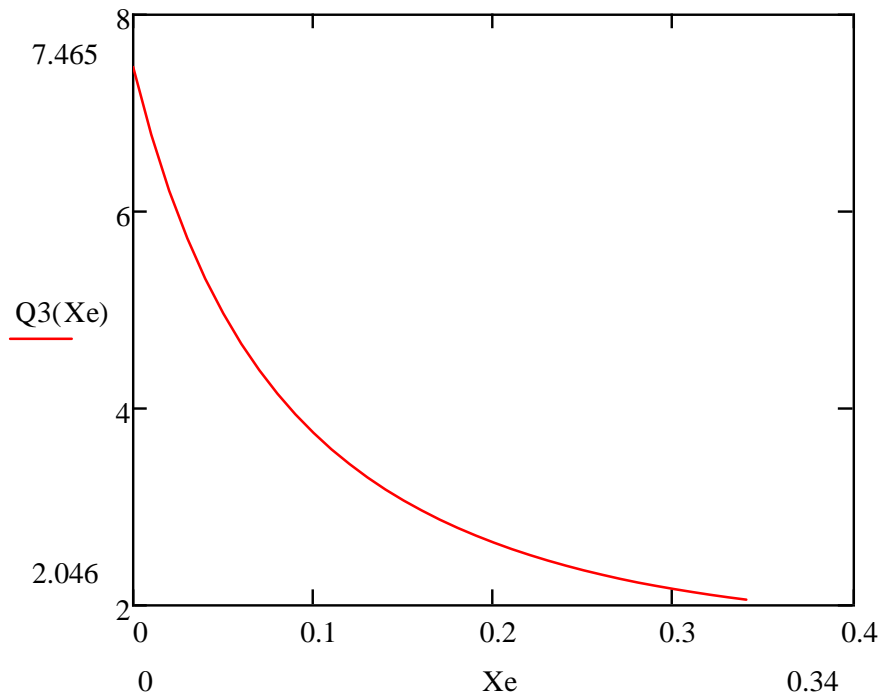


Figure 24 Heat value of the exiting gases at point 3.

Looking on the graph of Q_{net} we see that they follow the exact same curve and are only separated by a consistent shift of about 0.5 watts. Thus at very high flow rates, and as the graph shows, nearly all other flow rates, \dot{m}_2 and \dot{m}_1 tend to cancel through the heat exchange and leave $\dot{m}_3 * h_{3sp}$ as the dominating factor in heat input. Thus we can operate at very high flow rates and have an efficient outcome. This has the added benefit of lowering the necessary heating temperature, and thus lowers the specification temperature on exhaust heat in designing a plant for example. In reality though, the friction losses due to these high flow rates would most likely require us to operate at a lower exiting fraction.

We have a second primary way of increasing efficiency of the system. In most professional systems a water cooling system runs through the absorber to lower the temperature of the mixing ammonia and water. As was seen on the temperature vs. fraction diagram earlier in the paper, the amount of ammonia absorbed into water increases as temperature drops. This

can increase the incoming fraction of ammonia in the water. In theory this should allow us to lower flow rates further and thus heat input. Using our Mathcad file we altered our entering fraction X , and range of exiting fraction X_e , to 0.4737. This is the fraction of ammonia when the solution is cooled to the freezing point of water. Making those two simple changes we obtained:

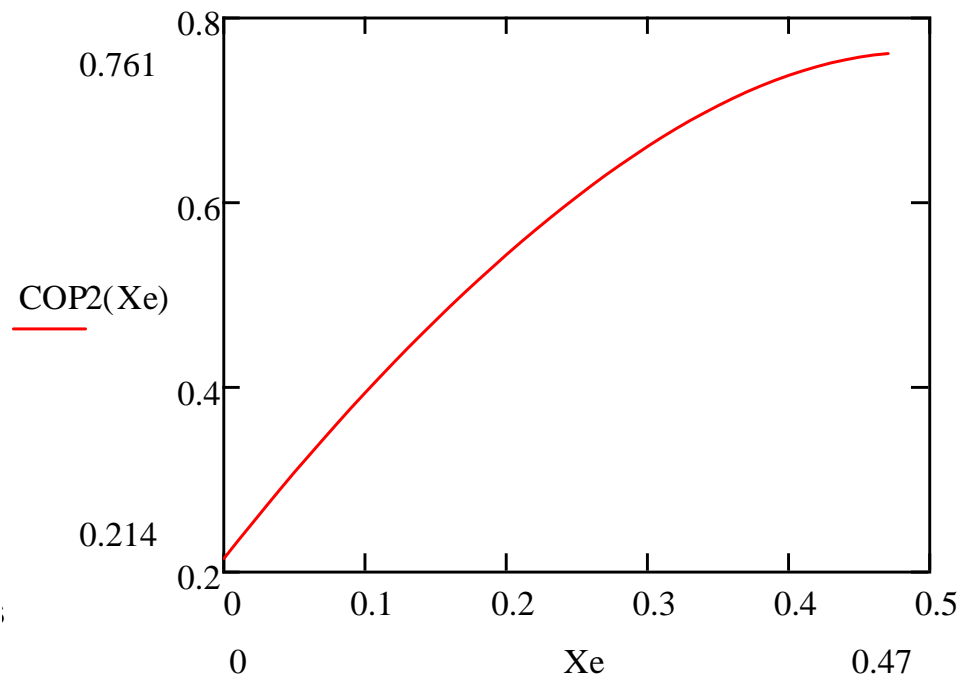


Figure 25 COP with heat exchange and solution pre-cooling .

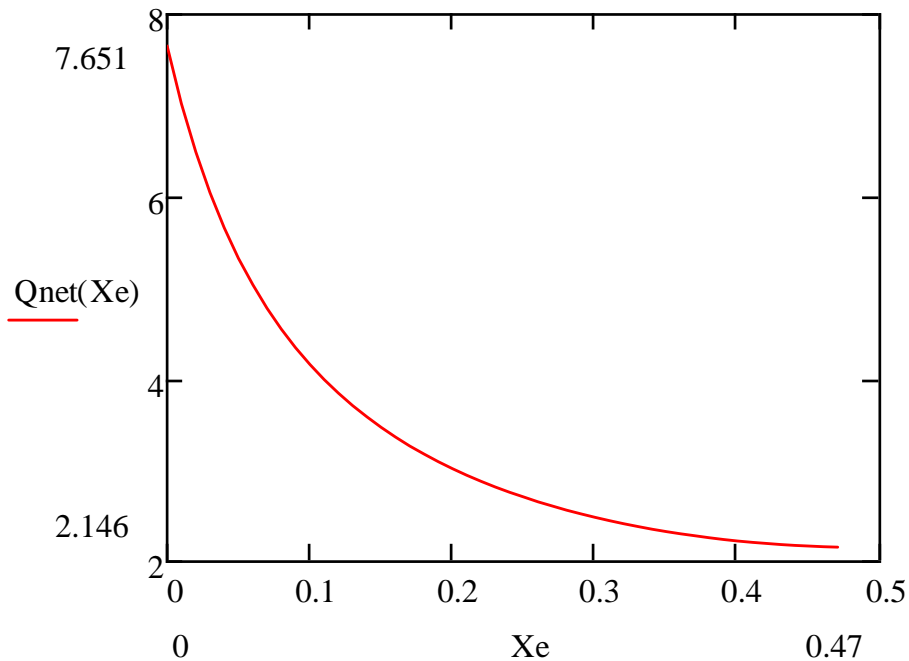


Figure 26 Net heat input with Heat exchange, and pre-cooling.

These two results are coupled with heat exchange. They thus represent the maximum theoretical system efficiency possible.

We obtain a similar curve to before with only heat exchange. Again the optimum occurs at the maximum fraction and highest flow rates. This is for the same reasons explained previously, the final enthalpy after cooling of the exiting flow at point 2 is nearly equal to that of the incoming solution at point 1. With \dot{m}_1 and \dot{m}_2 being very close in value, the heat exchange tends to cancel out; this leaves $\dot{m}_3 \cdot h_{3sp}$ as the only significant heat factor. The reason the higher initial concentration increases efficiency is that h_{3sp} decreases with increasing X_e . Thus, less heat and a lower temperature are required to produce ammonia vapor.

So, to summarize we have a tradeoff between heat exchange vs. mass flow vs. enthalpy. With no heat exchange an optimum will occur. This is the result of increasing enthalpy with decreasing X_e , and increasing mass flow with increasing X_e . When heat exchange is factored in, the max COP always occurs at $X_e = X$; slightly below it of course so as to not produce infinite

flow rates. This is because heat exchange reuses the solution heat at point 2 such that as X_e increases the heat of 2 and the needed heat of 1 cancel leaving $\dot{m}_3 h_3$ which drops with increasing X_e . Greater system efficiency is always obtained with the use of generator heat exchange and pre-cooling.

Comparison of Systems

Our above theoretical analysis confirms the numbers put forward in table 10 in our two-fluid absorption section. Examining this table we see that Ashrae's theoretical system achieves a COP of 0.571, with an entrance fraction of $X=0.5$, and an exit fraction of $X_e=0.41$. We stated above that the Δh_{sp} of heat exchange decreased as X_e increased. So to compare our theoretical model directly we alter our X 's to match Ashrae's example. It should be noted that Ashrae's theoretical model used an effectiveness for the solution heat exchanger. The correct exchanged heat is then simply given by:

$$Q_{exch(eff)} = \varepsilon Q_{exch}$$

We set ε to be 0.692 as table 10 specified, and then generated the following graph of COP.

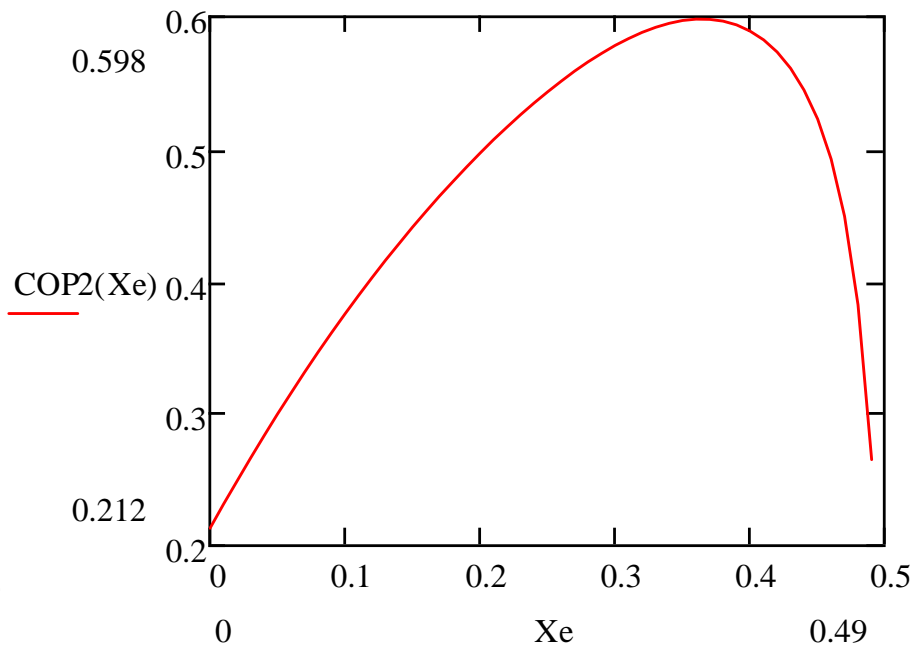


Figure 27 COP with heat exchange and pre-cooling. However, this chart includes a heat exchanger effectiveness of $\epsilon=0.692$.

The max COP of 0.598 is relatively close to Ashrae's values. Our model gives us a slightly lower exiting fraction of about 0.36 for the optimum. However, although it is not labeled we can see that COP is roughly 0.57 at the $X_e=0.41$ mark. So our result falls closely in line with Ashrae's model. This could indicate that Ashrae's system is not being operated at the optimum point due to other factors. Looking through table 9, we see that they have made most of the same ideal assumptions that we have. Pipes and pumps are isentropic, the expansion valves are adiabatic, and the liquid solution exiting the generator is at its saturated value of enthalpy. Although, we do not have pumps and valves in our system it works out to create the same model.

There is one further efficiency measure that we have not included. Ashrae's, and most, absorption systems use refrigerant heat exchange in addition to generator solution heat exchange. Refrigerant heat exchange cools the refrigerant exiting the condenser at ambient temperature with the cool refrigerant exiting the evaporator. This pre-cools it before entering and eliminates

unnecessary heat transfer in the refrigerator. We have not included it in our model as we do not have a typical system with an expansion valve as theirs does. That being said, our theoretical results match theirs relatively well.

There is one more problem yet unsolved in analyzing the system however. Our model has been intended to create a model of generator heat input without taking the remainder of the system into consideration. The absorber-generator-condenser portion of a three fluid and two fluid system are roughly identical when considered under ideal circumstances as our model and Ashrae's are. The results of our model are confirmed by Ashrae's example as well as others we have examined in *Absorption Chillers and Heat Pumps* by Herold, Radermacher, and Klein. So we have successfully, though this is ultimately the reader's interpretation, created a relatively accurate model of heat input into any ideal absorption system. By using heat exchange and cooling water to increase X , we increased our theoretical performance to a max of 0.761. Yet, in practice typical gas absorption systems do not exceed a COP of approximately 0.3. What is the reason for this discrepancy.

The reason is that evaporation process in a gas absorption system is not the same as that of a vapor-compression or two fluid absorption systems. Ammonia is not alone; it occupies the evaporator with hydrogen. In addition, as was explained before, the ammonia does not evaporate by the standard process of absorbing heat by virtue of a lower temperature. It seeks equilibrium with its vapor phase and increases its partial pressure in the hydrogen until it reaches equilibrium. This is a different process and cannot be modeled in the typical way. We have used a standard evaporator analysis for our Mathcad model in order to compare it the standard absorption system. The true heat drawn into the evaporator is much higher than the heat transferring through the box. Thus the COP of a gas absorption system drops due to the

numerator value, not the denominator which is generator heat input. This is a consequence of operating with a single system pressure.

We have one additional reason worth mentioning. We have shown that when heat exchange is included it is preferable to operate with higher mass flows and more heat exchange. But in a three fluid system we have no electronic or mechanical components. If we want to increase mass flow we must input more heat to run the bubble pump more quickly. In a two fluid system we can increase electric power to the pump to increase flow rate, so we do not have that problem. As a result of this mass flow limitation we are restricted to lower flow rates and lower COP's. Most commercial units operate between 0.05 and 0.2 exiting mass fraction X_e . Commercial units also include heat exchangers. Looking back to figure 27, which includes heat exchange with effectiveness and pre-cooling, we see that we are limited to a COP of about 0.35 at $X_e=0.1$. So, without taking any non-idealities into account we can still see why we are limited to such low COP's. It is primarily a combination of the non-equilibrium evaporation process, and the mass flow limitations of the generator.

DETERMINATION OF MASSES

The final portion of our analysis remaining is to determine the masses of each of the three fluids needed to operate the system. The three fluids needed are water, hydrogen, and ammonia. To determine their masses requires primarily knowledge of the system's components' volumes, and the density of each fluid.

We initially set up a general equation for determining the masses. Mass is given by the following equation:

$$M = \rho * V$$

This is simply density times volume. We then needed to determine the volume of each component of the system. Some components such as the evaporator and condenser can be determined exactly, as they have precise specifications which we will follow during construction. Other components such as the bubble pump tube, hydrogen gas return pipe, water return pipe, and U-bend sections, are somewhat arbitrary in shape and dependent upon the circumstances encountered during construction. Their volumes will have to be estimated to the best degree possible.

Hydrogen Mass

Hydrogen occurs in the following sections of the system: evaporator, absorber, and hydrogen gas return pipe. The evaporator volume is known and fixed at a volume of: $V_e = 0.0000824 \text{ m}^3$. The absorber and hydrogen return pipe are unknown as they may alter for construction reasons. We will label them V_{abs} and V_{hr} for now. Next we need the density of hydrogen in each section. In the evaporator we have based our partial pressure on an overall hydrogen pressure of 6.448 bar. Since density varies with temperature and pressure we analyze densities when the system is at rest at room temperature. When the system is not operating, all fluids will end up at room temperature. We can analyze gas density based on the pressure assumed for that section and room temperature. For hydrogen in the evaporator this results in:

$$P = \rho * R * T$$

$$\rho = \frac{P}{R * T}$$

$$P = 644,800 \text{ N/m}^2$$

$$R_h = 4124 \text{ J/kg} \cdot \text{K}$$

$$T = 293.15 \text{ K}$$

$$\rho = .5334 \frac{\text{kg}}{\text{m}^3}$$

In the absorber we assume that most of the ammonia gas is still present, and hydrogen is at the same pressure and thus the same density. In the return pipe, the ammonia has absorbed leaving approximately 90% hydrogen. Based on this pressure we get a density of:

$$\rho = .7444 \frac{\text{kg}}{\text{m}^3}$$

Now, we sum densities and volumes to obtain total mass:

$$M = \rho_e * V_e + \rho_{abs} * V_{abs} + \rho_{hr} * V_{hr}$$

This will be done after construction and volume testing is completed.

Ammonia:

Gaseous ammonia mass is determined in much the same way. We find the volumes of each component it occupies, and the densities in those volumes. The ammonia occupies the evaporator, condenser, absorber, and hydrogen return pipe. The evaporator and condenser have volumes of $8.24\text{E-}5\text{m}^3$ and $1.44\text{E-}4\text{m}^3$, with the other volumes determined after construction. In the evaporator we take the mean ammonia pressure to be 3.552 bar. In the condenser it is at 10bar, in the absorber 3.552 bar, and 1bar in the return pipe. We assume that the great majority of the condenser volume is gaseous and neglect the small fraction of its volume that may be occupied by liquid ammonia. Using $R_{amm}=488.2\text{J/kg} \cdot \text{K}$, and evaluating densities we obtained.

$$\rho_{cond} = 6.897 \frac{kg}{m^3}$$

$$\rho_{evap} = 2.482 \frac{kg}{m^3}$$

$$\rho_{abs} = \rho_{evap}$$

$$\rho_{hr} = .7 \frac{kg}{m^3}$$

Our ammonia gaseous mass then becomes:

$$M = \rho_e * V_e + \rho_{abs} * V_{abs} + \rho_{hr} * V_{hr} + \rho_{cond} * V_{cond}$$

Liquid Ammonia Hydroxide:

The densities of the gases are on the order of 100 times less than those of liquids, and in our system most of the volume is taken up in the absorber and generator sections due to their large dimensions. Thus, the great majority of the mass in our system is found in the liquids. The liquid ammonia hydroxide occupies half the absorber, all of the generator and half the bubble pump tube at rest. At room temperature the density of ammonia hydroxide is 865.4 kg/m^3 . Upon determination of the volumes, the total liquid mass will be:

$$M_{tot} = \rho_{sol} * V_{abs-gen}$$

After this mass is found and computed we must then find the mass of each component. This can be done by using our mass fraction equation from the previous generator analysis section:

$$0.342 = \frac{M_a}{M_{tot}}$$

Where 0.342 is the fraction of ammonia at room temperature, and M_{tot} is the total solution mass given above. We then simply solve for M_a , and subtract it from M_{tot} to get the mass of water.

We will of course need to make minor adjustments for sections such as the water return pipe and any length that is altered during construction.

PART DESCRIPTION

When choosing our piping we initially decided to go with threaded pipes for our use, but as we looked we found that the fittings for most of the pipes did not meet our pressure rating requirements. The operating pressure of our refrigeration cycle is 10 bar or 145 psi. This means that all of the components must be rated to a bursting pressure of at least 580 psi because operating pressures should be 25% of rated bursting pressures. We previously chose a 1/4 inch 312A stainless steel schedule 40 piping which is rated to 24,444 psi and has a wall thickness of 0.088 inches. This schedule 40 piping vastly exceeds the strength needed, but with such a substantial wall thickness it would have been difficult to mold into the coils and various other bends in our system. After much deliberation we met with Neil Whitehouse, the Higgins Shop Lab Machinist. He highly recommended using automotive brake line tubing. 3/8 inch steel brake line tubing is much more practical, with a bursting pressure rating of roughly 5300 psi and a wall thickness of 0.028 inches. Brake line tubing fittings are rated to a much higher pressure than threaded pipe fittings because the tubing is flared on each end and thus does not use the same threaded fitting as the schedule 40 pipe. The flared brake line tubing is also less expensive than the threaded schedule 40. Steel brake line tubing is clearly a better choice than the threaded piping. Flared automotive brake line tubing is produced in two types. One with the ends flared at a 37 degree angle, and one with ends flared at a 45 degree angle. Each is suitable for our system

and would work equally well. The initial problem was that it was nearly impossible to find the complete set of stainless steel tubing and fittings in either flare type needed for our system. Stainless steel 45 degree flare fittings and stainless steel 37 degree flare tubing are extremely rare. It took a great deal of probing to locate a compatible combination of tubing and fittings, but once we altered our material to steel the problem subsided.

Choosing the tanks for our system was unique in comparison to the choosing rest of the parts. Pressure tanks or cylinders are not in high demand and are usually put to use in custom applications. There is no industry standard, so selecting a uniform type and size of a tank was not possible. We eventually found a tank from Advanced Specialty Gases that met all of our design requirements, except cost. It would not corrode in the presence of ammonia, and is small and strong enough. A lower priced option was found, however. For the generator, absorber, and separator tanks we decided on carbon steel schedule 40 pipe with butt-welded end caps. The capped pipes will perform identically, but for roughly half the cost.


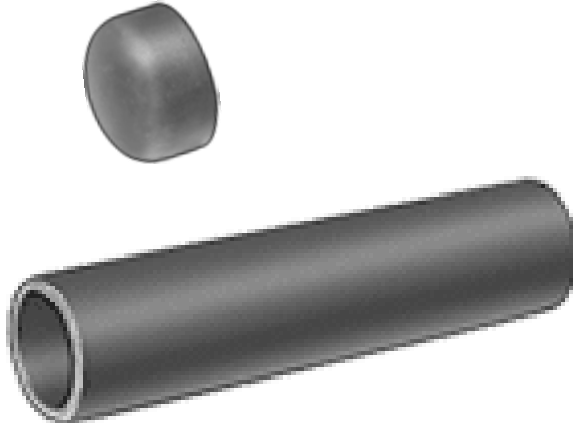

To ensure that the system functions correctly, temperature and pressure measurements need to be taken. Therefore, gauges need to be installed and must be made of steel as well. A pressure gauge is needed to monitor the system pressure when filling the system with the chemicals and to confirm that the system is not leaking the refrigerant. A device to display temperatures in the generator is also necessary to regulate the heat input. We originally intended to use stainless steel dial thermometers, but decided to use thermocouples instead because they are a fraction of the cost and are precise enough for our purposes. We intend to find both thermocouples on campus free of charge.

Another feature that would have been extremely beneficial to include is some sort of apparatus that allows visual observation of the inside of the system. This could have aided

greatly in the trouble shooting process, providing the liquid level in the absorber tank and enabling the view of the refrigerant supposedly traveling through the system. Unfortunately, after thorough research we were unable to find any aforementioned device that could be implemented in our system. All of the possibilities, such as high pressure glass tubing and windowed pipe fittings are hundreds of dollars out of our price range. Having a completely closed system with no visual vantage points to the inside of the system may become a huge problem if the refrigeration cycle does not initially operate as predicted, but we were left with no choice.

In order to fasten all of these portions of the system together, numerous fittings are necessary. A fitting is a part that can attach two or more sections of piping or tubing. Flare nuts are mandatory on the end of every connecting tube; partnering with the fitting heads to create the seal. A tubing sleeve is added between the tubing nut and the tubing to provide additional support to the flare. Steel flare T-fittings will be needed at all locations in the cycle where three tubes unite. A steel threaded-to-flare adapter fitting is going to be used to connect the pressure gauge into the system. The gauge employs a threaded connection that must be converted to become integrated into the system. Initially, steel flare couplings were intended to be welded into holes in the sides of all the tanks in order to connect the tubing. Upon arrival, the couplings were deemed to be not robust enough to undergo the welding process without melting and distorting. Instead, we chose female threaded weld bungs to weld into the tank holes. These required male threaded to flared adapters to screw into the female threads, providing a flared fitting for the tubing. Couplings will still be used everywhere that two tubes conjoin in the system, however. Various other adapter fittings and T-fittings will be needed to incorporate the input, bleeding, and flow restricting valves, but these fittings have not yet been decided upon

Table 1. Parts images.

<p><u>6 ft. Steel Flare Tubing:</u></p>  <p>http://www.inlinetube.com/Straight%20Length/straight.htm</p>	<p><u>Tank Piping and Caps:</u></p>  <p>http://www.mcmaster.com</p>
<p><u>Stainless Steel, Liquid Fillable Pressure Gauge:</u></p>  <p>http://www.omega.com/ppt/pp/tsc.asp?ref=PGM_Series&ttID=PGM_Series&Nav=</p>	<p><u>Thermocouple:</u></p> 
<p><u>Steel Female Threaded Weld Bung</u></p>	<p><u>Steel Flare T-Fitting:</u></p>



http://www.lightningmotorsports.com/vibrant/vibrant_weld_bungs/g-54374.aspx



<http://www.mcmaster.com/#flared-tube-fittings/=fdjs7n>

Steel Female Threaded-to-Flare Adapter Fitting:



<http://www.mcmaster.com/#flared-tube-fittings/=fdjzv4>

Steel Male Threaded-to-Flare Adapter Fitting



<http://www.mcmaster.com>

Steel Flare Coupling:



<http://www.mcmaster.com/#flared-tube-fittings/=fdjtmn>

Steel Flare Nut:



<http://www.mcmaster.com/#flared-tube-fittings/=fdk8ck>

Steel Flared Fitting Cap



<http://www.mcmaster.com/#standard-flared-tube-fittings/=ghrvby>

Steel Tubing Sleeve:



<http://www.mcmaster.com/#flared-tube-fittings/=fdkdrn>

Part Prices

			Unit	Total
Model or Part #	Item Description:	Qty:	Price:	Price:
50695K164	Male threaded to flared adapter	8	\$2.03	\$16.24
50715K514	Flared fitting cap	1	\$7.49	\$7.49
50695K282	T-fitting	6	\$8.60	\$51.60
50695K262	Coupling	12	\$1.74	\$20.88
50695K173	Female threaded to flared adapter	1	\$2.63	\$2.63
50695K226	Tube nut	20	\$1.12	\$22.40
50695K218	Tube sleeve	20	\$0.79	\$15.80
7750K118	Steel pipe: 12" length, 3" diameter	2	\$31.57	\$63.14
7750K119	Steel pipe: 12" length, 4" diameter	1	\$38.43	\$38.43
43425K186	3" steel end cap	4	\$17.51	\$70.04
43425K216	4" steel end cap	2	\$25.34	\$50.68
	6' segment of steel tubing	7	\$21.50	\$150.50
9768688	Stainless steel pressure gauge	1	\$36.71	\$36.71
11272	3/8 inch female weld bung	8	\$5.04	\$40.32
Total:				\$586.86

CONSTRUCTION

The initial phase of the construction process was to find and purchase materials. In order to do this, we first mapped out all of the design parameters and requirements. All materials had to meet or exceed every requirement to ensure safety and the proper function of the system.

Tools necessary for construction included: a hand held tube bender, tube flaring kit, wrench, hacksaw, metal file, drill press, and welding equipment.

The majority of our refrigeration unit consists of flared automotive brake line tubing. Instead of using elbow fittings and various other types of joints to shape our system, we used a tube bender to bend the tubing into our desired figure. A tube bender is a relatively small tool that resembles a pair of pliers. As shown in Figure 28, you simply place the portion of the pipe

that you wish to bend into the tube bender and force the tube around the rounded component to the desired degree.



Figure 28 Hand held tube bender

<http://www.northerntool.com>

Using a tube bender not only saves money on extra fittings, but allows us to mold the tubing exactly to our needs. It enabled us to create all of the custom shapes in our design, such as the spirals for the condenser and the evaporator.

To add another degree of control we personally cut all of the tubing to the lengths found in our calculations. A common hacksaw easily cut through the steel tubing, which was then filed on the newly cut surface to remove imperfections and smooth out the rough edges. Both the metal file and the hacksaw can be seen respectively in Figure 29.



Figure 29 File and hacksaw

<http://www.ehsmith.co.uk>

<http://community.craftsman.com>

The cut edge was then flared to connect to a fitting. A flaring tool uses a combination of vises to forcefully expand the diameter of the end of the tube into what is called a flare. The end of the tube was placed between two parts of the flaring tool that clamp together around the tube, holding it firmly in place. Then a tapered piece is forced into the tube by another vise, stretching or flaring the end. Figure 30 shows an example of a flaring tool and a flared tube end.

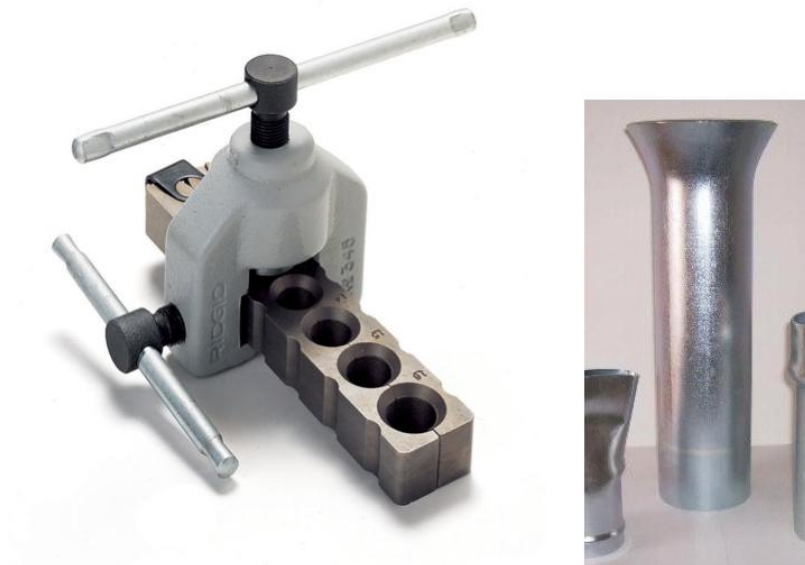


Figure 30 Flaring kit and flared tube end

<http://www.ridgid.com>

<http://www.techniswage.co.uk>

Cutting the tubes to length and flaring the ends ourselves allows for all of the tube segments in the cycle to be exactly as designed. We did not have to settle for predetermined tube length or pay extra for customized sizing.

Once all of the tubing was the correct shape and size the assembly process began. The flared steel tubing was connected using flared steel fittings. The fittings attach to the tubing using threads, but the tubing itself is not threaded. Two female nuts and sleeves are mounted on to the tubing before it is flared. The nuts and sleeves are free to slide on the tubing, but the flares at each end prevent them from being removed. To connect the tubing to the fitting a nut and sleeve was moved to the end of the tube. The sleeve rests inside the nut, while its only purpose is to add strength to the joint. Figure 31 contains a picture of a flared T-fitting and an illustration of a flared fitting junction.

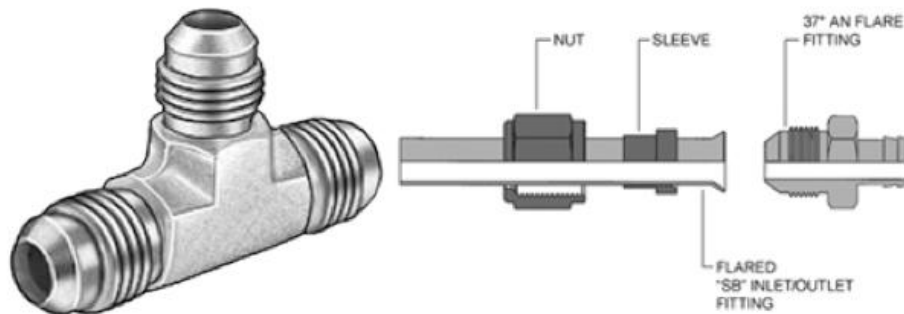


Figure 31 Flared T-fitting and junction assembly

<http://www.mcmaster.com>

<http://www.lytron.com>

The nut's threading reaches over and past the tube flare, where it meets the male threading of the flare fitting. The flare fitting has a tapered end that fits inside the tube flare. When the nut is tightened it sandwiches the sleeve and tube flare between it and the fitting, creating the seal.

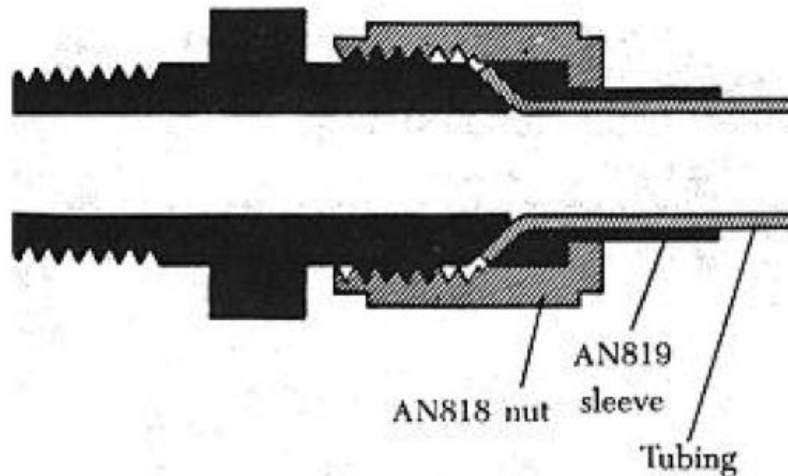


Figure 32 Flared tube connection illustration

<http://avstop.com/ac/apgeneral/plumbingconnectors.html>

The construction process was completed without any major drawbacks. A few minor unforeseen challenges forced the final refrigerator structure to deviate from the original design dimensions slightly. These small changes should not affect the operation of the refrigeration cycle. Apart from that, the fabrication progressed as expected.

The first and most serious oversight was the connection of the tubing to the tanks. Originally, the plan was to weld flared coupling fittings into holes in the tank walls, allowing a connection for the tubing on both the outside and inside of the tank. This would enable the bubble pump tube to extend inside the separator tank so that the heated solution could pool in the bottom. After consulting with our welder, we were advised that the difference in wall thickness of the coupling and the tank would cause the coupling to melt during the welding process. The problem was solved by purchasing female threaded weld bungs and corresponding adapters. However, this would not allow tube connection inside the separator tank, which prevented liquid

pooling in the separator. We averted this setback by modifying the bubble pump to enter the separator from the side, rather than the bottom. The bubble pump is now the same height as originally planned, but a different length, because a 90° bend was added to enable the horizontal entry into the separator. The separator tank also had to be moved a few inches horizontally to account for the new configuration.

After the separator was moved closer to the absorber to fit the bubble pump, the space for the u-bend connecting the absorber tank and the separator became limited. Initially we did not realize that this would be a problem. It became apparent when attempting to bend the tubing into shape that the tube bender did not have a small enough bending radius to form the u-bend in the space available. Multiple attempts were made, but the tubing would kink before the required bend was completed. This problem was easily solved. The tube linking the absorber tank to the generator tank was extended, which consequently distanced the separator and absorber tanks, providing enough space for the u-bend.

As stated before, these changes to the system are minor and should not negatively affect the operation of the cycle. Fortunately, no obstacles that required major design variations arose during the construction process. Figure 33 shows the completed system.



Figure 33 Picture of completed system

FILLING PROCEDURE

The filling of our system will require two entry locations built into the cycle. One will simply be a T-fitting between the generator and absorber tank to pour the water into with a cap to close. The other will be a valve between the separator and condenser to input the hydrogen, ammonia and air. No bleed valve is necessary because the capped T-fitting can be loosened to act as a bleed valve.

The system fill procedure will follow these steps:

- **Step 1: Measure the volume of liquid required to create the proper operating liquid level in the bubble pump and the total system volume.** The operating liquid level volume will be measured before the entire system has been assembled by adding water to a connection of the generator tank, absorber tank, and bubble pump. When the correct liquid level is reached, the water will be removed and measured. The same procedure will be followed to measure the total volume of the entire system.
- **Step 2: Purge all air from the system.** The system will be turned upside down and filled with water. Rotating the system may be required to bring all air bubbles to the fill point. The T-fitting will then be sealed with the cap and the system turned right side up.
- **Step 3: Remove excess water and add hydrogen.** The pressurized hydrogen tank will be connected to the top valve, and the cap on the T-fitting at the bottom of the system will be to allow water to leak out. The water leaking out of the bottom will be replaced by hydrogen at the top. The purpose of this is to ensure that no air is left within the system. The water leaking out will be measured and the cap tightened when the proper amount of water is removed from the cycle. The proper amount of water will be calculated by subtracting the operating volume of liquid from the total volume of the system found in Step 1. Hydrogen will continue to be added until the correct amount is reached. The correct amount

will be determined using Dalton's law of partial pressure at the equilibrium state.

The corresponding pressure of hydrogen at the non-equilibrium state will be calculated using the ideal gas law and the volume it will fill.

- **Step 4: Add desired amount of ammonia gas.** The desired amount of ammonia gas will be determined by the desired water and ammonia mixture chosen for system operation. Knowing the volume of the water left in the system, we can find the molar amount of water molecules, divide it by the desired concentration, and subtract that quotient to the molar amount of water molecules to obtain the molar amount of ammonia gas required. Using ideal gas law on the tank of ammonia gas, we can calculate the pressure rating of the calculated molar amount of ammonia gas.

SYSTEM SAFETY

Our system utilizes ammonia gas and hydrogen. Both of which have risks to using. Ammonia gas is toxic and can cause death by poisoning if the exposure to it is high enough. Hydrogen gas exposure has no significant risks, but it is flammable. However, hydrogen gas will never approach the heated sections of our system so this is not a significant concern. Our solution of ammonia-water has risks as well. If ammonia-hydroxide makes contact with the skin it can produce burning and discoloration. If somehow ingested, it has a range of bad effects all of which revolve around severe irritation and damage to organs. There is no reason why ammonia hydroxide ingestion should be a risk in our project however.

We begin our safety analysis by exploring corrosion rates. Ammonia gas is highly corrosive to certain metals, particularly copper. So we must select a safe material to use. At the

advice of professor Sisson we checked ammonia corrosion data in the book Corrosion data survey published by the National Association of Corrosion Engineers. The data in the book indicated that all stainless steels, as well as many cast irons, would handle pure ammonia gas safely up to a temperature of 260°C. This is sufficient, as our ammonia should reach about 200°C at maximum.

We examined next the data on ammonia water solution. At a concentration of 30-40% by mass in water the data indicated that solution would have a penetration rate into stainless steel of less than 0.02 inches per year up to a temperature of 93°C. Above this temperature data was not given. It can be assumed however that corrosion will increase with temperature since atomic diffusion accelerates with temperature. This will be an issue since we have a minimum operating temperature of 180°C in the generator tank and the wall thickness of our steel piping is 0.028 inches. The generator has a thickness of 0.25 inches, which is sufficient to be considered safe for our operating period.

A corrosion rate of .02 inches is very high relative to our wall thickness of .028 inches. This will cause a drop in pressure rating as it eats through the pipe. It appears that emptying of the unit may be a necessity after completion of the project. For the time being, we analyze the pressure stresses on the piping with reduced thickness due to corrosion. Considering the pipe to be thin walled we compute radial, tangential and axial stresses, in the wall of the pipe.

$$\sigma_t = P/t$$

$$\sigma_r = 0$$

with a pressure of 10 bar, a radius of .00476m, and a corrosion reduced thickness of .004 we get a stress of:

$$\sigma_t = 1,190,000 \text{ pa}$$

To find the maximum stress in an element of a material we compute the von misses stress. The von misses stress is the maximum stress produced in a plane direction on a differential stress element. It is given by the equation:

$$\sigma = \sqrt{\frac{(\sigma_x - \sigma_y)^2 + (\sigma_y - \sigma_z)^2 + (\sigma_z - \sigma_x)^2 + 6(\tau_{xy}^2 + \tau_{yz}^2 + \tau_{zx}^2)}{2}}$$

Since our only stress is tensile stress, which we can use as σ_x , we get a maximum stress of:

$\sigma = 1,190,000 \text{ pa}$, which is our computed stress because it is the only stress acting. We approximate radial stress as zero in a thin walled cylinder. Axial stress only applies in a closed ended cylinder.

Next we make corrections for the conditions of the piping operation. This is a series of correction factors that reduces the rated stress rating of a metal to a lower value based on its operating conditions. The series is given by:

$$S_e = C_{\text{load}} C_{\text{size}} C_{\text{surf}} C_{\text{temp}} C_{\text{reliab}} S_e^1$$

Each of the C terms is a fraction that reduces stress level. These five factors correct for type of loading, axial or moment, physical size of the part, surface roughness conditions, operating temperature, and reliability of the data. The final term is the original optimal stress rating.

Using steel data tables we see that stainless steel 316, has a ultimate tensile rating of 621MPa.

We multiply this by 0.5, for steels under a 1400 MPA rating, to get endurance strength.

Endurance strength is the stress level below which steel will have infinite life under cyclical

stress. However, we do not have cyclical stresses in our system so this is simply an extra margin of safety.

We compute Endurance strength to be 310.5 MPA. We then apply the series of corrections to obtain a maximum safe rating for stress. The process of determining the correction factors is somewhat long. The results of however are:

$$S_e = 84.5336 \text{ MPA}$$

This is the maximum allowable safe stress in the part after applying corrections for load type, size, operating temperature and reliability. As for reliability, this refers to statistical reliability of the data. We chose a reliability value of 99%, which gave us a correction factor of 0.814. Now, with our max safe stress, and computed max operating stress, we a safety factor of:

$$N = \sigma_{\max} / \sigma$$

$$N = 71.036$$

Even after one year's corrosion, we still are maintaining a safe level of stress. This is presuming the radial stress is zero. However we are unable to account for accelerated corrosion rates at 200°C because of a lack of current information. Given the large safety margin it will more likely than not be within tolerance after a year, nevertheless more data is required in the future. The possibility should be examined of using a thicker pipe for the sections exiting the generator, or a different material altogether.

All of the above is valid based on data by the national association of corrosion engineers. Many other sources indicate that in fact ammonia will not corrode carbon or stainless steel. In this case, we would use carbon steel as it is the more common of the two. This is based on data from the 2nd edition handbook of Corrosion data by the American Society of Materials, as well as the 1998 ASHRAE handbook. The corrosion data book indicated that neither stainless steel nor

carbon steel are affected by anhydrous ammonia or ammonia hydroxide. The book mentioned stress cracking at very high pressure for carbon steel under ammonia hydroxide, but this was typically only in the presence of humid air. Further, the ASHRAE handbook actually recommended Stainless Steel and Carbon Steel for ammonia systems. They also provided the appropriate schedule number for the carbon steel based on pipe diameter. For diameters below 1.5 inches they recommended schedule 80 carbon steel. Our piping does not have a schedule number. It is designed for brake lining and auto industry standards. But, it does have a more than adequate working pressure and burst pressure rating for our purposes. So the piping itself can be considered safe.

Our only concern is in the absorber, generator, and separator. Here we are boring holes and placing in weld bungs to connect our pipes. We have bored holes in the wall of our tubes and caps to place the bungs in. We are therefore altering the natural part from its prescribed operating ratings. We must account for this.

In the holes of the tube wall we are placing weld bungs in. The weld bungs will essentially act as a continuous portion of the tube once sealed in. There is no danger here of bursting. The same applies in the caps. We have welded holes in two of the caps, one in the top of the generator, and a second in the top of the separator. These should again be acting as a part of the continuous volume once welded in and should provide sufficient safety. In addition to the bungs, we are welding at the seal points of the cap and tube. These are designed to be welded and both the cap and tube have the same pressure ratings. So provided that the weld is of good quality these should not be a point of concern.

For the sake of safety we guess a weld thickness at the bungs of .028", the same as that of the piping. Thus is unrealistically low, but that is what makes a reasonable safety analysis

starting point. We then reanalyzed system stresses as previously to determine theoretical safety in the tanks at the weld bung/tank interface points. This time we did not use the thin walled approximation but the standard equations:

$$\sigma_r = \frac{P_i r_i^2 - P_o r_o^2}{R_o^2 - R_i^2} - \frac{r_i^2 r_o^2 (P_i - P_o)}{r_o^2 (r_o^2 - r_i^2)}$$

$$\sigma_p = \frac{P_i r_i^2 - P_o r_o^2}{R_o^2 - R_i^2} + \frac{r_i^2 r_o^2 (P_i - P_o)}{r_o^2 (r_o^2 - r_i^2)}$$

$$\sigma_a = \frac{P_i r_i^2 - P_o r_o^2}{R_o^2 - R_i^2}$$

with:

$$p_i = 10 \text{ bar}$$

$$p_o = 1 \text{ bar}$$

$$r_i = 0.032 \text{ m}$$

$$r_o = 0.0381 \text{ m}$$

We then modeled the interface as a bar in tension, as no closer model existed, and computed a stress concentration factor of 2.62. We then reapplied the von misses stress equation and obtained the following result:

$$\sigma = 27.1 \text{ MPA (Max theoretical stress)}$$

As before we applied correction factors for shape, temperature, machining, etc. These were

$$C_{\text{size}} = 0.781158$$

$$C_{\text{surf}} = 0.869$$

$$C_{\text{temp}} = 1$$

$$C_{\text{relib}} = 0.868$$

With a tensile stress for steel of 500MPa, taken as a lower value, we then used an endurance stress of 250MPa to compute safety. The result was:

$$N=103.1137153/27.1$$

$$N=3.804$$

So, our weld bung interface points should be safe. All that remains is to ensure that the weld is of good quality. Welding is currently still in progress.

TESTING AND MEASURING PROCEDURES

Volume Measurement

Two volume measurements were done on the system in order to get the proper liquid solution level in the absorber and bubble pump, and to calculate the proper amount of hydrogen and ammonia gas required for system operation. The solution level test was undertaken before the system was completely constructed. A visual example can be found in figure 34, below. To obtain the necessary solution mixture level, the absorber, generator, and bubble pump tube were connected to each other and filled with water up to the top of the absorber. The water was then drained and measured. This was conducted three times to ensure an accurate result. The three results, which differed less than 0.27%, were averaged. The average volume of the absorber divided by two, which was calculated using the same process beforehand, was subtracted from the total solution level volume, yielding the volume of solution required to generate our desired operating liquid level: 2.4 liters.

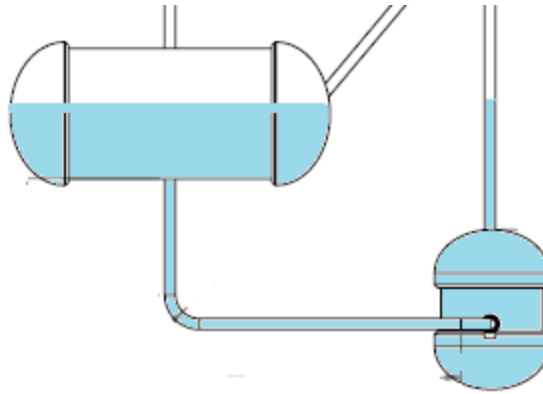


Figure 34 Illustration of operating liquid level

The volume measurement of the entire system was conducted after the whole system was assembled. Water was poured into the system through the gas valve connector point using the method of siphoning. Since the system has no other exit point to vent air, a connecting point near the top of our system had to be loosen in order to allow the air being displaced a place to escape. This point was retightened when the liquid level had reached that point, and water was fed into the system at a lower rate to minimize the bubbles created by the surfacing air. The system was then closed and tilted in all direction to allow any air in the bends to float to the top of the system and more water was added. This water was leaked though the cap opening at the bottom of the system into a beaker and was measured. The measurement of the required liquid solution level and that of the entire system were repeated 3 times and averaged for more accurate results.

Bubble Pump Testing

The bubble pump is the connector pipe between the generator and the separator. Its function is to facilitate the flow of ammonia vapor and the weak ammonia hydroxide solution out of the generator and into the evaporator. Without the bubble pump the system cannot function, so it was necessary to ensure that it functions properly. The bubble pump flow rate test was

conducted while only the absorber, generator and bubble pump were assembled. The system was filled to the operating liquid level and a propane torch flame applied to the bottom of the generator. After roughly ten minutes of heating, liquid began bubbling out of the top of the bubble pump. Five flow rate tests were conducted at lengths varying from one to two minutes.

Pressure Testing

The system was pressured tested for any leaks using air. The air was fed into the system through the gas intake connector slowly to an initial pressure of 50 psi and increased by increments of 10 psi. The initial pressure test at 50 psi revealed that there were leaks at every fitting. Water was sprayed onto the system connection points so that the escaping air produced bubbles, making it easier to spot leaks. Teflon thread seal tape was added to all fittings in the system to help seal the leaks after it was found to be non-reactive with ammonia gas or hydroxide (nibco, 2003). It was placed on all threads and between all flares and their fittings. There were no sign of leakage at 50 psi with the Teflon seal tape. The pressure was increased up to 97 psi with still no sign of leakage. The system was left at 97 psi overnight.

RESULTS

This section outlines the results of the test and measurements obtained for the required liquid solution volume, the total system volume, the bubble pump flow rate, and the pressure test using the procedures outlined in *The Testing And Measuring Procedures* section. It also gives the required fluid mass calculated using the measured volumes.

Liquid solution and total system volume

The average volume of the absorber was calculated using the same process used to calculate the total system volume, and half of that absorber volume was subtracted from the

measured volume spanning from the top of the absorber to the equivalent point in the bubble pump pipe to yield the required operating liquid level volume. The required liquid level volume was calculated to 2.4 liters. The total system volume was measured to be 5.425 liters.

Masses of all fluids

The masses of each fluid to be added were then found to be: 1.361 kg of water, 0.72461 kg of ammonia, and 0.8157 grams of hydrogen.

Bubble Pump Flow rate

After roughly ten minutes of heating, liquid began bubbling out of the top of the bubble pump. Five flow rate tests were conducted at lengths varying from one to two minutes. The liquid exited the bubble pump at an average temperature of 66 °C at an average rate of 78.3mL/min. This is much larger than our calculated flow rate of 7.19E-3 mL/min. The large flow rate found during testing is not foreseen to be a problem because the testing conditions deviate from the operating conditions. The test was done with the system open to the environment and at a temperature above 20 °C. At operating conditions of the system of 10bar of pressure and a temperature of 20 °C, the mass flow rate of the bubble pump is expected to be lower. The sole purpose of the bubble pump test was to ensure that it actually worked. Bubble pump testing was successful.

Pressure Test

For the last pressure test, the system was pressured with air at 97 psi and left overnight. Unfortunately, the pressure of the system had dropped to 77 psi the next day signifying that there were still some small leaks in the system. Further investigation has lead us to conclude that the small leaks in the system are most likely due to uneven flaring of the pipes using the flaring tools.

CONCLUSION

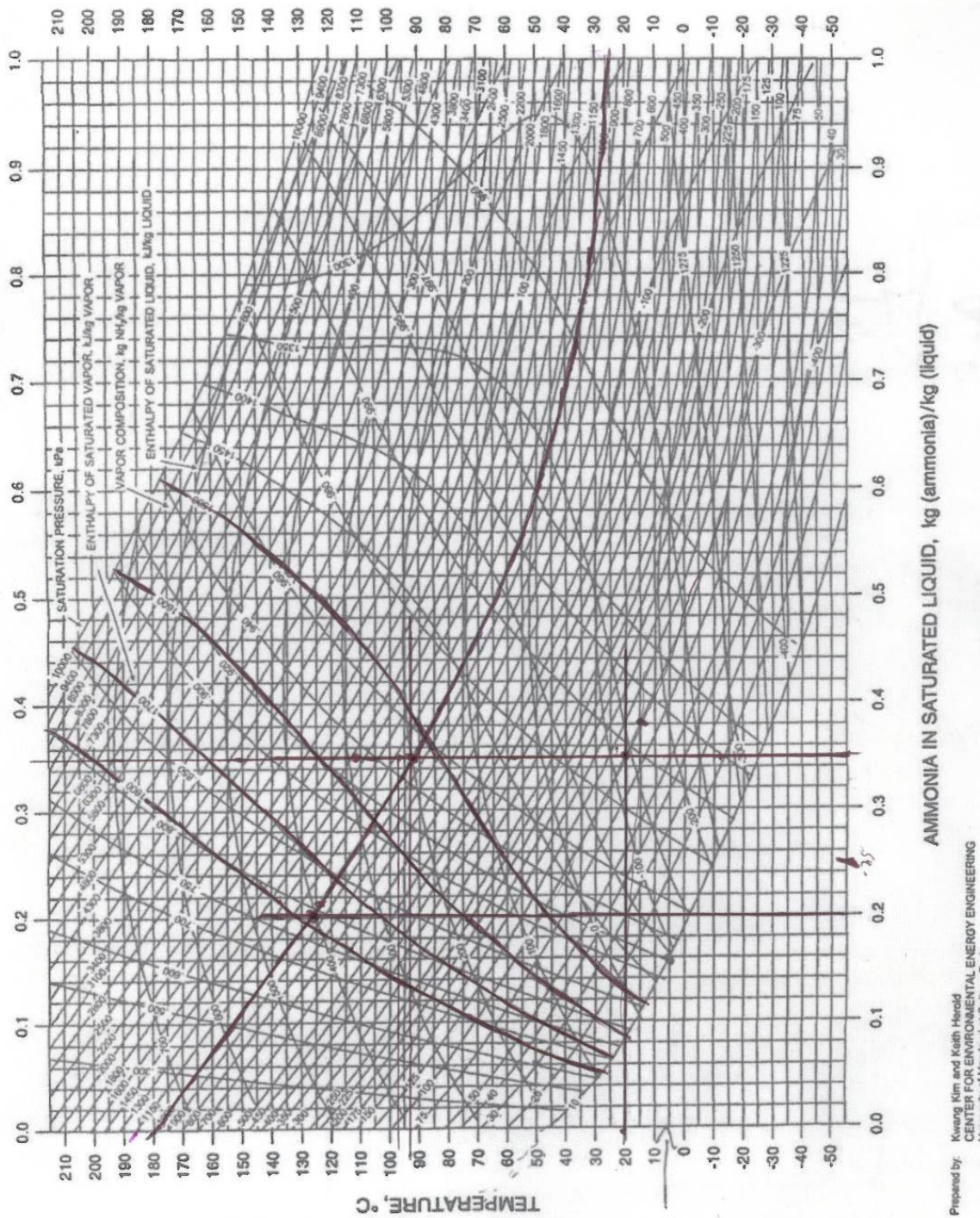
After the repair of the small leaks our three fluid absorption refrigeration will be ready for operation when the three fluids are added. 1.361 kg of water, 0.72461 kg of ammonia, and 0.8157 g of hydrogen should be introduced into the system using the procedure shown in the *Filling Procedure* section of this report. With the addition of a heating source, the system will cool our refrigerant compartment to 3°C at a surrounding temperature of 20°C and an internal pressure of 10bar. The system will last at least 6 months, but should not be operated over 1 year due to the corrosion of Teflon (0.02 in per year) by ammonia hydroxide.

We recommend that the flaring on the pipes be redone using a better and more precise tool than a manual flaring tool kit to ensure that there are no leaks. The chosen materials were designed to be assembled using flares while allowing no leaks under an internal pressure of 5000psi. With the proper flaring there should be no need for the Teflon tape and there should be no leaks.

This project offered a great opportunity to apply the concepts and knowledge acquired in the educational process at WPI. The MQP project at WPI is extremely valuable and a large portion of what sets WPI apart from average institutions. It integrates research, analysis, design, and practice to provide an accurate example of real world experience. Although this project was unable to be completed as originally intended, many skills specific to the professional field of study were still gained.

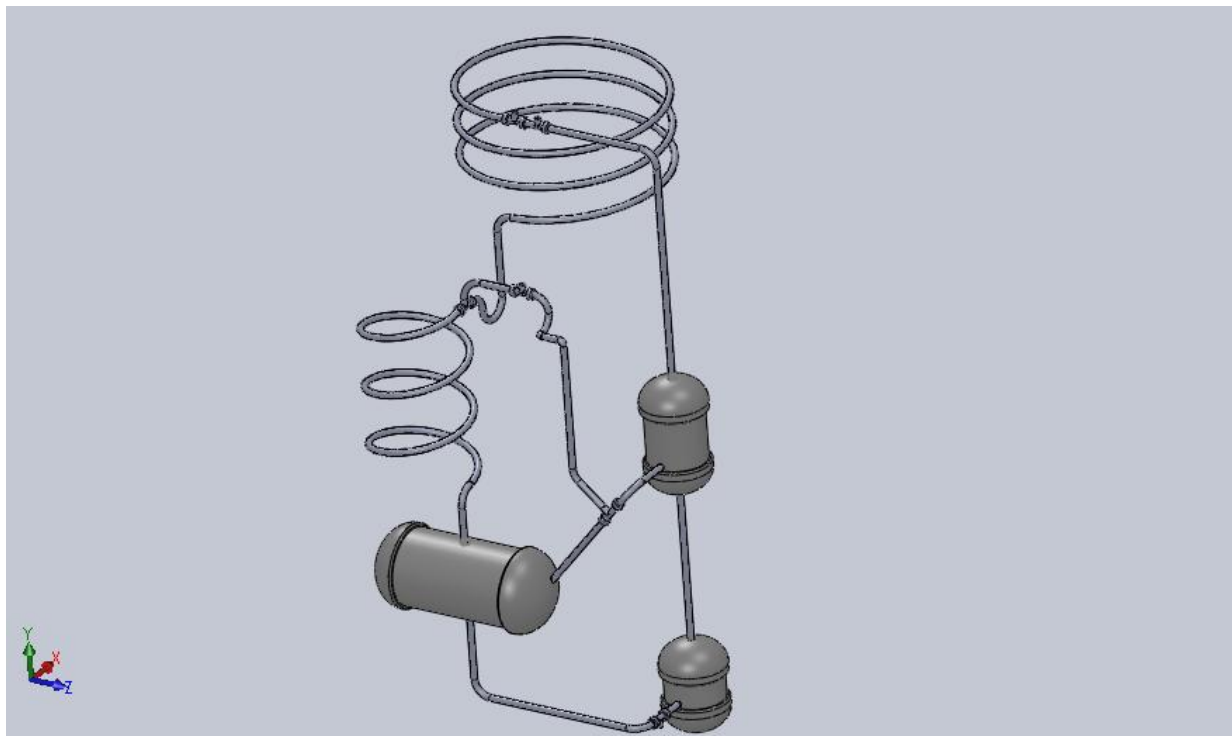
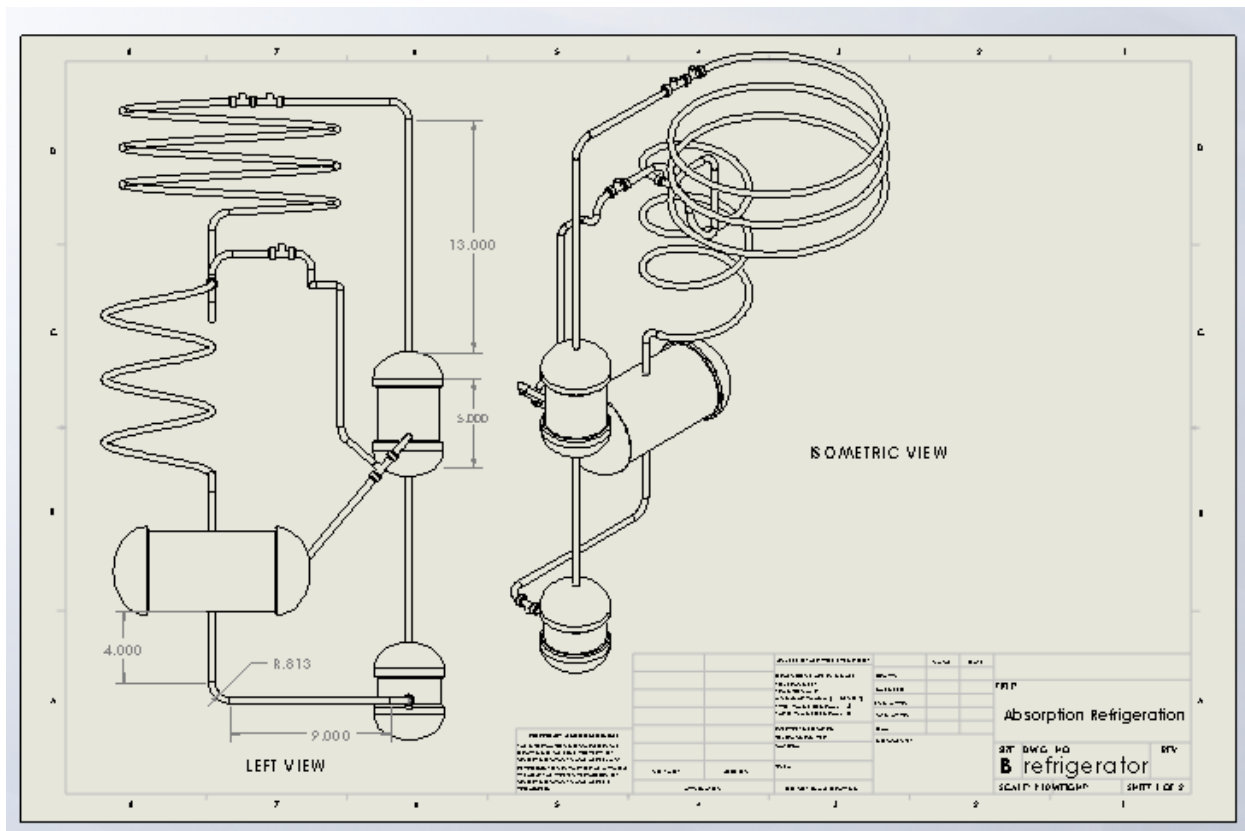
APPENDIX 1

Temperature-Enthalpy-Concentration Diagram



APPENDIX 2

Solid Works model of our system



APPENDIX 3

Set of equations from our MathCad file

$$X := .473$$

$$Xe := 0.01 \dots 473$$

$$mw := 100$$

$$m'a := .00000127$$

$$he := 1279.56100$$

$$h2(Xe) := \left[-\left(87891Xe^5 \right) + \left(102102Xe^4 \right) - \left(39760Xe^3 \right) + \left(7040.4Xe^2 \right) - \left(2322.5Xe \right) + 773.4 \right] \cdot 100$$

$$h3(Xe) := \left[-\left(51272Xe^5 \right) + \left(79849Xe^4 \right) - \left(57234Xe^3 \right) + \left(26914Xe^2 \right) - \left(8718.1Xe \right) + 2795.8 \right] \cdot 100$$

$$h1(X) := \left[-\left(36512X^6 \right) + \left(65948X^5 \right) - \left(52890X^4 \right) + \left(22791X^3 \right) - \left(4103.3X^2 \right) - \left(506.3X \right) + 90.444 \right] \cdot 100$$

$$h12(Xe) := \left[-\left(36512Xe^6 \right) + \left(65948Xe^5 \right) - \left(52890Xe^4 \right) + \left(22791Xe^3 \right) - \left(4103.3Xe^2 \right) - \left(506.3Xe \right) + 90.444 \right] \cdot 100$$

$$Xvi(X) := \left[-\left(20.522X^4 \right) + \left(29.507X^3 \right) - \left(19.128X^2 \right) + \left(6.6936X \right) + .0025 \right]$$

$$Xvf(Xe) := \left[-\left(20.522Xe^4 \right) + \left(29.507Xe^3 \right) - \left(19.128Xe^2 \right) + \left(6.6936Xe \right) + .0025 \right]$$

$$Xw := 1 - X$$

$$maf(Xe) := \frac{(Xe \cdot mw)}{(1 - Xe)}$$

$$ma(Xe) := \frac{[X \cdot mw + (maf(Xe)) \cdot (X - 1)]}{(1 - X)}$$

$$Xaf(Xe) := \frac{maf(Xe)}{mw + ma(Xe) + maf(Xe)}$$

$$m'w(Xe) := \frac{(Xw \cdot m'a)}{(1 - Xaf(Xe)) \cdot (1 - Xw) - (Xw)(Xaf(Xe))}$$

$$m'af(Xe) := \frac{[Xaf(Xe) \cdot (m'w(Xe) + m'a)]}{(1 - Xaf(Xe))}$$

$$Xa(Xe) := \frac{(ma(Xe))}{mw + ma(Xe) + maf(Xe)}$$

$$Xe2(Xe) := \frac{Xvi(X) + Xvf(Xe)}{2}$$

$$m'w(Xe) := \left(\frac{m'a}{Xe2(Xe)} \right) - m'$$

$$m'w_{\text{a}}(\text{Xe}) := \left(\frac{m'a}{\text{Xe}2(\text{Xe})} \right) - m'i$$

$$m'_{\text{3}}(\text{Xe}) := m'a + m'w_{\text{a}}(\text{Xe})$$

$$m'_{\text{2}}(\text{Xe}) := (m'w(\text{Xe}) - m'w_{\text{a}}(\text{Xe})) + m'af(\text{Xe})$$

$$m'l(\text{Xe}) := m'w(\text{Xe}) + m'a + m'af(\text{Xe})$$

$$Q(\text{Xe}) := m'_{\text{3}}(\text{Xe}) \cdot h3(\text{Xe}) + m'_{\text{2}}(\text{Xe}) \cdot h2(\text{Xe}) - m'l(\text{Xe}) \cdot h1(\text{X})$$

$$\text{COR}(\text{Xe}) := \frac{m'ahe}{Q(\text{Xe})}$$

$$Q3(\text{Xe}) := m'_{\text{3}}(\text{Xe}) \cdot h3(\text{Xe})$$

$$Q2(\text{Xe}) := m'_{\text{2}}(\text{Xe}) \cdot h2(\text{Xe})$$

$$Q1(\text{Xe}) := -m'l(\text{Xe}) \cdot h1(\text{X})$$

$$Q_{\text{exch}}(\text{Xe}) := m'_{\text{2}}(\text{Xe}) \cdot (h2(\text{Xe}) - h12(\text{Xe}))$$

With Heat Exchange:

Net Q with solution heat exchange

$$Q_{\text{net}}(\text{Xe}) := Q(\text{Xe}) - Q_{\text{exch}}(\text{Xe})$$

$$\text{COP}_{\text{2}}(\text{Xe}) := \frac{m'ahe}{Q_{\text{net}}(\text{Xe})}$$

$$Q_{\text{c}}(\text{Xe}) := m'_{\text{2}}(\text{Xe}) \cdot h12(\text{Xe}) - m'l(\text{Xe}) \cdot h1(\text{X})$$

WORKS CITED

ASHRAE Handbook Fundamentals, 1997 (IP). (1997). American Society of Heating.

chen, j., & Herold, K. (1995). *Buoyancy effects on the mass transfer in absorption with a nonabsorbable gas*. college park: university of maryland.

Chubu Electric Power Co., I. (2006, 11 07). *Development of Room Temperature Magnetic Refrigeration System*. Retrieved 04 02, 2012, from Chubu Electric Power:
http://www.chuden.co.jp/english/corporate/press2006/1107_1.html

Corrosion Data Survey 6th Edition. (1985). National Association of Corrosion Engineers.

Devotta S.A.V, W. N. (2001). *Alternatives to Air Conditioners*.

Engineers, A. S.-C. (1998). *1998 ASHRAE Handbook: Refrigeration*. Atlanta: ASHRAE.

Engineers, N. A. (1985). *Corrosion Data Survey Metals section sixth edition*. Houston: NACE.

Herold, Radermacher, & Klein, a. (1996). *Absorption Chillers and heat pumps*. New york: CRC Press.

Incroper, Dewitt, Bergman, & Lavine, a. (2007). *Fundamentals of Heat and mass transfer 6th Edition*. New Jersey: John wiley & sons .

Jernqvist, A. K. (1993). *International Journal of Refrigeration*.

Karonen, I. (n.d.). *Lecture 5: Heat Engines, Refrigerators, and the Carnot Engine*. Retrieved 04 02, 2012, from http://www.nhn.ou.edu/~jeffery/course/c_energy/energy1/lec005.html

koolatron. (n.d.). *THERMOELECTRIC REFRIGERATION*. Retrieved 04 02, 2012, from koolatron:
<http://www.koolatron.com/test/images/thermoelectric.html>

Krasner-Khait, B. (n.d.). *The Impact of Refrigeration*. Retrieved 2011 йил 10-11 from History Magazine:
<http://www.history-magazine.com/refrig.html>

Materials, A. S. (1995). *2nd Edition Handbook of Corrosion Data*. OHIO.

Moran, & shapiro, a. (2008). *Fundamentals of Engineering Thermodynamics 6th Edition*. New Jersey: John Wiley & sons.

Moran, M. (2008). *Fundamentals of Engineering Thermodynamics*. John wiley & son.

Norton, R. (2011). *Machine Design 4th edition*. Prentice Hall.

Organization, N. E. (2006 йил 7-11). *Development of Room Temperature Magnetic Refrigeration System* . Retrieved 2011 from Chubu Electric Power:
http://www.chuden.co.jp/english/corporate/press2006/1107_1.html

Solutions and Colligative Properties : Phase Diagrams. (n.d.). Retrieved 2012 йил 26-03 from Oracle ThinkQuest: <http://library.thinkquest.org/C006669/data/Chem/colligative/phase.html>

Vitalij K. Pecharsky, K. A. (1999, 12 09). Magnetocaloric effect and magnetic refrigeration. Ames, Iowa.

Zohar, Jelinek, and A. Levy, "The influence of Diffusion Absorption Cycle Configuration on Performance." *Applied Thermal Engineering* Volume 27 Issue 13 Sept. 2007: P. 2213-2219. SciVerse online. Web 2012